Reneau et al. 1996

45

ER ID# 56047

# Geochemistry of Background Sediment Samples at Technical Area 39

Steven Reneau, EES-1, Katherine Campbell, EES-5, Patrick Longmire, CST-7, and Eric McDonald, EES-1

JUL 2 3 1997
em

March 4, 1996 Revision

Chapter of LA-MS Report on Background Geochemistry at Los Alamos National Laboratory

P. Longmire, D. Broxton, and S. Reneau, Editors


## Summary

This report presents results of chemical analyses of 24 analytes in 16 background sediment samples collected from Ancho Canyon and Indio Canyon at Technical Area (TA) 39. Preliminary upper tolerance limits (UTLs) for sediments are calculated from this data set, but, because of the small sample size, these UTLs exceed the maximum values in the data set by up to 50%, and will require revision as more background sediment data are obtained.

Systematic variations in the background chemistry of sediments at TA-39 occur between different geomorphic settings and different particle sizes. These differences indicate that the best comparison of potentially contaminated sediments to background should utilize the most comparable subset of the background data set. The lowest concentrations of most analytes occur within coarse, well-sorted sands in active stream channels (which are dominated by quartz and sanidine crystals), and the concentrations of most analytes generally increase with decreasing sediment particle size. The concentration of U within one sample of black sand (dominated by high density magnetite grains) was within the range of other background samples. This relationship is important because the presence of higher concentrations of U in black sand deposits may thus indicate anthropogenic U that was concentrated by density as in a placer deposit.

Analyte concentrations in sediments are generally lower than those associated with B horizons in soils, but are comparable to elemental concentrations within the A and C horizons.


7396

However, the A and C soil horizons posses greater ranges, and thus use of UTLs developed for Laboratory soils may not be appropriate for evaluating potential contamination within sediments. Concentrations of elements in the sediments are strongly influenced by the total surface area available for adsorption, and concentrations of trace elements are minimal within the medium- and coarse-grained sediments with low surface areas relative to silt and clay. Different minerals concentrated in the sediments, such as magnetite, however, are higher in trace elements resulting in part from ionic substitution within the mineral lattice during primary crystallization. For example, a sample of magnetite-rich black sand is higher in As, Be, Cr, Mn, Ni, Pb, Th, U, V, and Zn relative to silicate-rich sediments.

Correlations exist between concentrations of different metals in the sediment samples (i.e., Fe and As, Fe and Be) that are similar to those present in soils at the Laboratory, although the concentrations of metals in the sediments are generally less than in the soils. Relationships between Fe and other metals of concern can be used to evaluate whether anomalously high values in a data set are within background ranges or instead may reflect contamination.

Concentrations of many analytes from sampled prehistoric channel and floodplain sediments are higher than their concentrations in more recent deposits, possibly caused by post-depositional additions of solutes associated with shallow groundwater flow within the alluvium. The processes that apparently increased concentrations of some trace elements within the prehistoric deposits may be similar to the processes affecting old sediments beneath the valley floor penetrated in core holes, suggesting that higher concentrations of many trace elements might be encountered in the subsurface than in surface sediment samples.

Principal components analysis (PCA) indicates that 89% of the variability in the background sediment data set can be accounted for by a single component, which is due to the strong correlations that occur between many major and trace elements. The remaining 11% is almost entirely accounted for by a second component that separates the two sample areas in Ancho and Indio Canyons. These results are similar to those obtained by PCA of the background soil data set of Longmire et al. (this report), for which overall variability is dominated by strongly

correlated variation of several major and trace elements, reflecting differences between soil horizons, and variation between sample sites is the second most important source of variability.

## Introduction

Sixteen sediment samples were collected from Ancho and Indio Canyons, TA-39 (Fig. 1), in August 1994 to provide background chemical concentrations from deposits comparable to those collected as part of Field Unit 2 (OU 1132) site characterization activities in Ancho Canyon. TA-39 has been used as a high-explosives firing site since 1953, and contaminants of potential concern that may have dispersed during experiments include Ba, Be, Cr, Pb, Tl, and U (LANL, 1993).

Two primary sample areas were chosen to increase the chance that the range of variability in natural sediment deposits were included and that any unanticipated contamination would be detected. The main sample areas are Indio Canyon, the largest drainage basin in the Laboratory entirely within Bandelier Tuff that has had no Laboratory facilities, and a small tributary to Ancho Canyon near State Road 4 that also has no upstream Laboratory activities (Fig. 2). An additional sample site is a stream bank along Ancho Canyon that exposes prehistoric (1000-3000 year old) sediments, which was chosen to evaluate whether such old deposits could also be used to provide valid background values. Sampled deposits were chosen to maximize the natural variability that exists within these sediments, and to evaluate systematic variations in chemistry that may exist between different geomorphic settings (i.e., channel vs. floodplain; Fig. 3) and between different size fractions. Descriptions of the samples analyzed in this study are presented in Table 1. Although we cannot be certain that all of the sampled sediments (particularly the active channel samples) have not been affected by airborne dispersion of contaminants from firing sites, procedures that we use to exclude outliers from the data set are expected to remove any potentially elevated analytes.

One limitation of this sampling program is the small size of the sample set from any specific geomorphic setting or type of deposit (i.e., coarse sands in active channel), at most two per sample set. These data, therefore, may not encompass the full range of variability that exist in sediments at TA-39. However, there is generally an internal consistency in this data set and systematic

variations exist between settings and size fractions, suggesting that this limited data set may be generally representative of similar settings in drainage basins underlain entirely by Bandelier Tuff.

## Laboratory Methods

Sediment samples were dried at low temperature in a laboratory oven and sieved to remove gravel (>2 mm) and roots. Splits of two large floodplain samples were dry sieved to separate the samples into three different size fractions: 0.25-2 mm (coarse and medium sand), 0.075-0.25 mm (fine sand), and <0.075 mm (very fine sand, silt, and clay). Clumps of sediment were manually crushed, but no chemical dispersants were used and the larger size fractions may therefore contain small portions of finer particle sizes.

Sample splits of all sediment samples were subject to three laboratory pretreatment procedures: partial digestion using nitric acid ($HNO_3$) at pH 1 (using standard extraction and analysis procedure specified in EPA Method 3050), which simulates the bioavailability of elements by humans through ingestion; leaching with deionized water, for analysis of easily dissolved Cl and $SO_4$; and complete digestion using hydrofluoric acid (HF), to provide whole-sample elemental concentrations. Analysis of As was by electrothermal vapor atomic absorption (ETVAA); of Cl and $SO_4$ by ion chromatography (IC); of Ta, Th, Tl, and U by inductively coupled plasma mass spectroscopy (ICPMS); and the remainder by inductively coupled plasma emission spectroscopy (ICPES). Results of the chemical analyses are presented in Tables 2, 3, and 4.

## Quality Assurance Checks

Sample splits of two bulk floodplain samples were submitted for analysis to provide an independent quality assurance (QA) check of the reproducibility of the analyses. For the combined 92 duplicate analyses of 24 analytes from the two sets of paired samples and two sample digestion procedures, 87 of the duplicate analyses (95%) were within the reported uncertainty, and three of the remainder (3%) were within twice the reported uncertainty (analyses of Al, Be, and Ni for one of the sample pairs). Only two sets of analyses (2%) were not consistent within twice the reported uncertainty, As and Ta for the paired samples FS2229 and FS2232. Overall, these results

therefore indicate that the laboratory analyses can be considered reproducible within the reported uncertainties.

## Comparison of Channel Samples and Floodplain Samples

Significant differences in analyte concentrations are present between the samples of coarse channel sands and the bulk floodplain samples, as summarized in Tables 5 and 6. For nearly all analytes, concentrations are higher in the floodplain deposits than in the channel deposits, as shown for As, Be, and U in Figure 4. This is consistent with the dominance of quartz and sanidine phenocrysts derived from the Bandelier Tuff within the channel deposits, and with the higher concentrations of fine-grained sediment in the floodplain deposits that could both have greater mineralogical variability (including higher abundances of clay minerals and ferric oxyhydroxides) and larger amounts of adsorbed trace elements. These differences indicate that the most precise evaluation of the presence or absence of contaminants within sediment samples and their possible concentrations should consider the geomorphic setting and associated particle size of the sediment samples. Specifically, lower natural concentrations of U, Be, and other analytes should be expected in the channel sands than in the floodplain deposits, and concentrations of these elements within potentially contaminated channel sediments should be compared to their concentrations in similar coarse-grained background samples and not the full data set.

## Analyses of Black (Magnetite-Rich) Sands

One sample of relatively clean black (primarily magnetite, $Fe_3O_4$) sand from Indio Canyon was analyzed to examine the natural elemental concentrations within these heavy mineral deposits. Field measurements of one black sand deposit near a TA-39 firing site had indicated above background radioactivity, and laboratory X-ray florescence (XRF) analyses of a sample from this site confirmed high concentrations of U (217 ppm; Ed Essington, unpublished data, 1994). It was thus hypothesized that such black sands may concentrate some anthropogenic heavy metals such as U as a "placer" deposit, and that selective sampling of black sands could provide an additional tool to examine the transport of high-density contaminants away from firing sites.

The sampled black sands from Indio Canyon (FS2225, Tables 2 and 3) have very high concentrations of many elemental species, including the highest concentrations of Fe, Mn, Sb, Th, V, and Zn from the $HNO_3$ digestion and Cr, Mn, Ni, Sb, Th, V, and Zn from the HF digestion (the low reported value of Fe in the HF digestion is believed to be due to laboratory error). Notably, although the concentration of U in the black sands was higher than in the typical channel sands, it was within the range of analyses from the floodplain samples. This indicates that where concentrations of U in black sands exceed the range of background floodplain samples, anthropogenic U may be present, and supports the hypothesis that depleted uranium particles from firing sites can be concentrated downstream in black sands due to sorting of sediment particles by their respective densities during transport by surface water.

In addition to U, many other analytes are also present in higher concentrations in the black sands than in other sediments in these canyons. As an example, Figure 5 shows the elemental concentrations for the black sands and the bulk sediment samples collected within the active channel deposits in Indio Canyon. These differences in elemental concentrations indicate the importance of mineralogy in influencing trace element distributions in heterogeneous sediments. The ratio of the elemental concentration in the black sands to the concentration in nearby channel deposits varies greatly between elements, and these ratios ($HNO_3$ digestion) in decreasing order are: V (47) > Zn (33) > Mn (23) > Be (17) > Cr (12) > Th (10) > Ni (9) > U (5) > As (4) > Pb (3). The higher concentrations in the magnetite-rich sands occur as a result of ionic substitution of the trace elements with one or more major elements within the mineral lattice during primary crystallization (Bloss, 1971) and/or adsorption onto secondary alteration products such as ferric oxyhydroxides (Rai and Zachara, 1984).

## Comparison of Different Size Fractions Within Floodplain Samples

Two large samples of floodplain deposits, one each from Ancho and Indio Canyons, were separated into three different size fractions to further examine the relation of particle size to elemental variability. A comparison of the elemental concentrations in these separates with the coarse channel sands (Tables 7 and 8), reveal several notable points.

Concentrations of most analytes progressively increase from the coarse channel sands to the fine sand separate, although element concentrations in the fine sands are generally indistinguishable from the very fine sand, silt, and clay fraction. These variations support the general increase in trace element concentration with decreasing grain size as indicated by the comparison of the channel sands with the bulk floodplain deposits. The similarity of the two finer size separates, however, suggests either that they are mineralogically similar or that they have similar adsorptive properties. Specifically, the percentage of clay minerals in these samples is unknown, and it is possible that they have very low clay contents, being dominated by very fine sands and silts that are geochemically similar to the fine sand fractions. For example, grain size analysis of a texturally-similar floodplain deposit overlying the sampled prehistoric channel sands in Ancho Canyon indicate the presence of only 8-9% clay-sized particles, compared with 26-44% silt and 47-66% sand (Bw1 and Bw2 horizons of Longmire et al., this report, Ancho Canyon site). Alternatively, because chemical dispersants were not used to disaggregate clays, it is possible that the coarse size fractions include aggregates of silt and clay or thin clay coatings on larger sediment particles. The higher analyte concentrations in the coarse and medium sand separates than in the channel sands suggest that the latter are perhaps better sorted, containing a higher percentage of quartz and sanidine crystals from the Bandelier Tuff, and also suggest that the coarse and medium sand separates may provide an analog with less well sorted channel deposits (with a higher content of fine sediment).

## Mud Deposit

One sample of a one-day old mud deposit from a flood in Indio Canyon (FS2226, flood of August 24, 1994) was collected as a possible fine-grained end member of natural sedimentary deposits in this environment. This deposit has the highest concentrations analyzed for several elements, including Al, Ba, Be, Ca, Mg, Na, Pb, and U for the $HNO_3$ digestion and Ta, Tl, and U for the HF digestion (Tables 2 and 3). Comparisons of concentrations of As, Be, and U in the mud deposit with channel and floodplain deposits are shown in Figure 4. For several analytes, the mud deposit exceeded element concentrations in the fine floodplain fractions taking into account the

analytical uncertainties. These analytes are Be, Cu, Pb, and U for both the $HNO_3$ and HF digestion and also Na for the $HNO_3$ digestion. Some of the elements that are high in the partial ($HNO_3$) digestions may reflect the presence of dissolved components that had been deposited at this site by evaporation, followed by precipitation and/or adsorption of solutes onto silt- and clay-sized sediments. Another possible complication with this deposit is that the proximity of State Road 4 may be responsible for the anomalous presence of certain elements derived from automobile exhaust, such as Pb. The high concentrations of other elements, such as U, may be more likely due to their adsorption onto silt- and clay-sized particles, although part of the U and other elements may be anthropogenic, dispersed from the TA-39 firing sites (see discussion in Longmire et al., this report, concerning possible anthropogenic U in surface horizons of some mesa-top soils).

## Comparison of Modern Sediment Samples and Prehistoric Samples

Samples of prehistoric sediments exposed in a stream bank along the main fork of Ancho Canyon were analyzed to test the hypothesis that prehistoric sediments could provide a reasonable local background in areas where adequate local background samples could not otherwise be obtained from active channels and floodplains because of the possibility of contamination by Laboratory operations. Alternatively, these samples may be more comparable to sediments penetrated at depth in a core hole than to surface samples because of post-depositional geochemical changes associated with prolonged contact with shallow groundwater or moisture within the vadose zone. Erosion of the sampled stream bank along the main drainage of Ancho Canyon exposed a section of coarse channel sands and gravels overlying an older floodplain deposit, shown schematically in Figure 3. Radiocarbon dating of charcoal contained within these sediments provided ages of about 1200 yrs for the channel sands and about 3200 yrs for the underlying floodplain deposit, demonstrating their prehistoric age.

Analyses from the prehistoric sediment deposits (FS2227 and FS2228) were compared to both the modern bulk channel and floodplain deposits and to appropriate size fractions from the separated floodplain deposits to ensure that possible natural variability within the modern deposits

was being considered (Tables 9 and 10). The prehistoric channel sands were thus compared with the medium and coarse sand fractions of the floodplain deposits, and the prehistoric floodplain deposits were compared with the fine sand to clay fractions of the modern floodplain deposits.

This comparison indicated that for most elements the modern and prehistoric samples could not be distinguished, but that for some elements significant differences exist that suggest post-depositional elemental mobility over the last 1000 to 3000 years. The old channel sand deposit in particular differed from both the modern channel deposits and also the medium and coarse sand fraction of the floodplain deposits (Fig. 6) with higher concentrations of Co, Cr, Fe Mn, V, and Zn in both the $HNO_3$ and the HF digestions, Ba, Ca, Mg, and Ni in only the HF digestion, and Cl and $SO_4$ in the deionized water leachate. As compared to the finer fractions of the recent floodplain deposits, the old floodplain deposits had higher concentrations of Na in the $HNO_3$ digested fraction and Cl and $SO_4$ in the deionized water leachate.

The differences seen between the modern and the prehistoric deposits suggest which elements may be naturally higher in subsurface samples collected from boreholes due to solute transport, mineral precipitation, and adsorption processes. Notably, some elements that are potential contaminants of concern at TA-39, such as Be and U, are similar between the recent and the old deposits, suggesting that natural concentrations of Be and U in the subsurface may be similar to those in young deposits. However, because of the small size of the data set (only one sample each of prehistoric channel and floodplain deposits), these inferences should be considered preliminary at this time.

The comparison of modern and prehistoric deposits suggests that the use of prehistoric sediment samples as a local sediment background in potentially contaminated canyons may be defensible in some circumstances, although care should be used in such an approach. Specifically, we expect that the older the deposit, the greater the chance for significant changes in chemistry due to post-depositional migration of certain elements, and information on the age and potential alteration of sampled sediments would thus be useful. However, this may only be a significant concern for a limited number of analytes, and the use of procedures that exclude outliers from the

background data set before summary statistics are calculated can minimize the effects of post-depositional elemental mobility on calculation of a sediment background.

## Arsenic and Beryllium in Sediments

Arsenic and Be are of special concern at the Laboratory in evaluations of possible contamination because their concentrations in soils routinely exceed action levels established by the Environmental Protection Agency (EPA) (0.32 ppm for As and 0.14 ppm for Be, using $HNO_3$ digestion) (Longmire et al., 1995). As a result, the evaluation of As and Be in soils at the Laboratory currently uses local background values to establish action levels, and background values thus play a key role in the decision making process. The analytical data obtained in this study similarly show that concentrations of As and Be in the sediment samples exceed the previously established action levels, although their concentrations in sediments are generally less than observed in local soils.

The concentrations of As and Be are generally strongly correlated with Fe concentration in soils at the Laboratory (Longmire et al., 1995, this report), and these elemental relationships are also present in the sediments collected within Ancho and Indio Canyons. Figures 7 and 8 are bivariate plots of As versus Fe and Be versus Fe for these sediments, showing high regression coefficients ($r^2$) of 0.84 and 0.95, respectively. These plots are useful in defining the background concentrations of As and Be as they relate to Fe concentration. Outliers to these bivariate plots may indicate contamination as opposed to natural variations in background concentrations of these analytes.

## Comparison With Background Soils

The background sediment samples from Ancho and Indio Canyons were compared with background soils data from the Laboratory (Longmire et al., 1995) to evaluate if the sediment chemistry was similar to certain parts of the soil data set. In general, elemental concentrations in the sediments are most similar to soil samples that contained low concentrations of Fe. In the soils, Fe concentration is generally correlated with the percentage of clay-sized particles in each

sample (Longmire et al., 1995), and the lower elemental concentrations present in the TA-39 sediments are consistent with their relatively low Fe content. For example, bivariate plots of As versus Fe and Be versus Fe for background soils and sediments collected at the Laboratory are shown in Figures 9 and 10. Arsenic, Be, and Fe concentrations in the sediments are most similar to concentrations within A and C horizons or within weakly developed B horizons in soils, although the A and C horizons show a greater range of As and Be concentrations. We thus infer that either the dominant source for the sampled sediments is erosion of soils containing low concentrations of Fe, or that much of the fine-grained Fe-rich component of the soils is winnowed out of the sediments during transport in floods, being carried downstream towards the Rio Grande. The differences between the sediment data set and the soils data set, including the greater range of values in the A and C soil horizons, indicate that it is not appropriate to apply UTLs developed for Laboratory soils to sediment samples.

## Principal Components Analysis

Patterns within the background chemical data set can be examined using a principal components analysis (PCA) (Everitt and Dunn, 1991). PCA helps to simplify the presentation and evaluation of a large multivariate data set by reducing its dimensionality. This simplification enables us to further evaluate, both qualitatively and quantitatively, the factors controlling the variability within the sediment data, and also the differences and similarities between the background soil data of Longmire et al. (this report) and the background sediment samples of this report.

The set of measured concentrations for a single sample constitutes one observation that is a vector in a 21-dimensional space, where each element listed in Table 2 corresponds to a dimension. After eliminating Cl and $SO_4$ (which are mostly below detection level), the black sand and prehistoric channel samples (which are distinctly different from the other samples), and also some of the major elements (Ca, K, and Mg) in order to minimize problems with singularities in the covariance matrix, there are still 16 dimensions, which are not easily visualized. However, virtually all (98.5%) of the variability among the remaining 14 observations occurs in a two-

dimensional subspace of this 16-dimensional space. A projection of the observations onto this subspace (Fig. 11) is very useful in determining what is controlling the variability among the samples.

In Figure 11, the x-axis (first principal component) corresponds to the direction in the 16-dimensional space along which the observations vary most (89% of the total variability). This first component separates the finest and intermediate size fractions (with higher concentrations of most elements) from the coarser fractions of the floodplain samples, and clearly isolates the channel sand samples (with relatively low concentrations) on the left side of the figure. As the PCA calculation was done without rescaling the observations, this first principal component reflects primarily variation in concentrations of the major elements, aluminum and iron.

It would also appear from Figure 11 that the bulk Ancho Canyon floodplain samples had more fine and medium material than the bulk Indio Canyon samples. The Ancho Canyon bulk samples plot on the right with the finer fractions, but the Indio Canyon samples are farther left. Overall, this first dimension of the PCA shows that size fractionation is the principal controlling factor in determining differences among the samples included in this study.

The second dimension, plotted on the y-axis of Figure 11, separates the two principal locations, Ancho and Indio Canyons. For this data set, the difference in chemistry between the sample sites in these two canyons is apparently the second most important factor in controlling the variability in chemical concentrations.

The projections of the two samples excluded from the calculation of the principal components in Figure 11, the prehistoric channel sand sample and the black magnetite sand sample, are way off scale on this plot, demonstrating how different they are from the remainder of the samples.

When principal components analysis is performed using data for the background soil samples of Longmire et al. (this report), the first two dimensions capture about 96.5% of the total variability and serve principally to separate the B horizon data from the A and C horizon data (Fig.12). The lower left-hand corner of this plot is occupied exclusively by samples identified as coming from the A and C horizons, although some samples from these horizons are scattered

farther up and to the right. When the sediment samples are projected onto these principal components, the sands and coarse fractions wind up within this lower left-hand corner, and the remaining samples (excepting, again, the prehistoric channel sands and the magnetite sands) are nearby. Overall, these plots further indicate that the sediment samples are most similar to soils from the A and C horizon, although the sediment samples are also similar to some of the B horizon samples, and the greater range for the A and C horizons limits their applicability as a substitute for sediment samples.

## Summary Statistics For Background Sediment Samples

Summary statistics for the sediment data are presented in Tables 11 and 12. In view of the fact that sample location is the second most important explanatory factor for the variation in observed concentrations, as shown by the principal components analysis, the sediment data discussed in this report should be considered strictly preliminary. Two sample areas are probably insufficient to represent the variability that will be encountered when more background sediment locations from other parts of the Pajarito Plateau are added.

This caveat should be borne in mind when using the statistics shown in Tables 11 and 12, which include medians, means, standard deviations, minima, maxima, and (.95,.95) UTLs based on the 16 sediment samples. The UTLs are calculated following procedures discussed in EPA (1989), and indicate values that we are 95% confident exceed the 95th percentiles of the true distributions. The statistics were calculated based on values from all samples, excluding outliers in the data set that would inflate the estimate of the mean by more than 10%, or, in the case of K, an anomalously low value. These outliers are presented in Table 13, and include values for the black magnetite-rich sands, the recent mud deposit, and the prehistoric channel deposits. The UTLs in Tables 11 and 12 are up to 50% larger than the maximum values observed, as a result of the small sample size, and will require revision as more background sediment samples are obtained.

## Implications for Sampling and Interpretation of Data

The data set discussed in this report is limited by its small sample size, and thus may not be representative of the full range of background sediment chemistry present at TA-39. In addition, this data set is not intended to be representative of all sediments on the Pajarito Plateau as the sampled canyons entirely drain areas underlain by the Bandelier Tuff. For example, additional variation will undoubtedly occur in the canyons that head in the Sierra de los Valles and thus drain areas underlain by Tschicoma Formation dacite. However, the results of this study suggest several implications for the collection of samples and the interpretation of analytical data that should allow improved evaluations of potential contamination in sediments at the Laboratory.

First, because of the dependence of sediment geochemistry on grain size and mineralogy, notes on the characteristics of each sample (such as the general grain size or the presence of black sands) can be valuable in understanding variations in the analytical data, and should be routinely made in the field by the sampling team. Second, the correlations that are present between Fe and other metals can be used as an additional test for possible deviations from background, such as for high values that may lie beyond the background data set but still be consistent with the natural elemental trends. Third, selective sampling of certain types of deposits (such as black magnetite-rich sands where dense particles like depleted U may be concentrated) may be useful in examining the transport of specific contaminants. Finally, sediments in the subsurface sampled in core holes may have significantly higher concentrations of certain elements than surface sediment due to post-depositional alteration associated with migrating water, and selection of appropriate background samples for comparison needs to be made accordingly.

## Acknowledgments

This work was supported by the Framework Studies Program and the Earth Science Technical Council of the Environmental Restoration Project, in close coordination with the OU 1132 (FU 2) field team. We thank Jamie Gardner and Everett Springer for their support, and Ed Essington for discussions concerning OU 1132 sediment sampling efforts. Lara Heister assisted with the field work and laboratory sample preparation, and CST-3 performed the chemical analyses. Dave Broxton, Ed Essington, and Randy Ryti provided helpful reviews of this report.

## References

Bloss, F. D., 1971, Crystallography and Crystal Chemistry: New York, Holt, Rinehart and Winston, 545 p.

Everitt, B. S., and Dunn, G., 1991, Applied Multivariate Data Analysis: New York, Halsted Press.

EPA (U.S. Environmental Protection Agency), 1989, Statistical Analysis of Ground-water Monitoring Data at RCRA Facilities. Interim Final Guidance: Office of Solid Waste, Waste Management Division, U.S. Environmental Protection Agency, Washington, D.C., April 1989.

LANL, 1993, RFI Work Plan for Operable Unit 1132: unpublished report, Los Alamos National Laboratory.

Longmire, P., Reneau, S., Watt, P., McFadden, L., Gardner, J., Duffy, C., and Ryti, R., 1995, Natural background geochemistry, geomorphology, and pedogenesis of selected soil profiles and Bandelier Tuff, Los Alamos, New Mexico, 1995: Los Alamos National Laboratory Report LA-12913-MS (in press).

Longmire, P., McDonald, E., Ryti, R., Reneau, S., and Watt, P., Natural background geochemistry of selected soil profiles, Los Alamos, New Mexico: (this report).

Rai, D., and Zachara, J. M. 1984, Chemical attenuation rates, coefficients, and constants in leachate migration, Volume 1: A critical review: Electric Power Research Institute Report EA-3356, Richland, Washington.

## Figure Captions

Figure 1. Location map of TA-39.

Figure 2. Location map of background sediment sample sites in Ancho and Indio Canyons. Site numbers referenced to samples in Table 1.

Figure 3. Schematic sketch showing geomorphic setting of background sediment samples. Approximate ages of sediments are from radiocarbon analyses of charcoal collected from Ancho Canyon sample site (site 4 of Fig. 2).

Figure 4. Comparison of the concentrations of As, Be, and U between floodplain deposits (sample FS2220), active channel deposits (sample FS2224), and mud deposits (sample FS2226) in Indio Canyon. Concentrations obtained using $HNO_3$ digestion (Table 2).

Figure 5. Comparison of the concentrations of selected elements in black, magnetite-rich sands (sample FS2225) and nearby active channel sands dominated by quartz and sanidine crystals (sample FS2224) in Indio Canyon. Concentrations obtained using $HNO_3$ digestion (Table 2).

Figure 6. Comparison of the concentrations of selected elements in prehistoric sands (sample FS2228) and active channel sands (samples FS2224 and 2233). Concentrations obtained using $HNO_3$ digestion (Table 2).

Figure 7. Plot of As vs. Fe for background sediment samples in Ancho and Indio Canyons (excluding samples FS2223, 2225, 2228, and 2232). Concentrations obtained using $HNO_3$ digestion (Table 2). Error bars indicate reported analytical uncertainties.

Figure 8. Plot of Be vs. Fe for background sediment samples in Ancho and Indio Canyons (excluding samples FS2223, 2225, 2228, and 2232). Concentrations obtained using $HNO_3$ digestion (Table 2). Error bars indicate reported analytical uncertainties.

Figure 9. Plot of As vs. Fe for background sediment samples in Ancho and Indio Canyons (excluding samples FS2223, 2225, 2228, and 2232), and the A, B, and C horizons of background soils at the Laboratory (Longmire et al., 1995). Concentrations obtained using $HNO_3$ digestion (Table 2).

Figure 10. Plot of Be vs. Fe for background sediment samples (from active channels and floodplains) in Ancho and Indio Canyons (excluding samples FS2223, 2225, 2228, and 2232), and the A, B, and C horizons of background soils at the Laboratory (Longmire et al., 1995). Concentrations obtained using $HNO_3$ digestion (Table 2).

Figure 11. Sediment samples from Ancho and Indio Canyons displayed in a coordinate system defined by their first two principal components. Note the breaks in the x and y axes that

indicate the locations of the black sand sample and the prehistoric channel sample, which have extreme values in this data set. See text for discussion.

Figure 12. Background soil samples of Longmire et al. (this report) and sediment samples of this report displayed in a coordinate system defined by the first two principal components of the background soil data set. Note the break in the y axis, and the extreme location of the black sand sample.

## List of Tables

Table 1. Location of sample sites and description of samples, TA-39.

Table 2. Chemical data for samples, TA-39, $HNO_3$ digestion.

Table 3. Chemical data for samples, TA-39, HF digestion.

Table 4. Chemical data for samples, TA-39, deionized water leachate.

Table 5. Summary of background sediment analyses, TA-39, $HNO_3$ and deionized water digestion.

Table 6. Summary of background sediment analyses, TA-39, HF digestion.

Table 7. Summary of different size fractions, TA-39, $HNO_3$ and deionized water digestion.

Table 8. Summary of different size fractions, TA-39, HF digestion.

Table 9. Comparison of modern and old deposits, TA-39, $HNO_3$ and deionized water digestion.

Table 10. Comparison of modern and old deposits, TA-39, HF digestion.

Table 11. Summary statistics for background sediment samples.

Table 12. Estimated summary statistics for selected radioactive isotopes in background sediment samples.

Table 13. Outliers in background sediment data set.

Table 14. Correction factors used to estimate concentrations of selected radioactive isotopes.

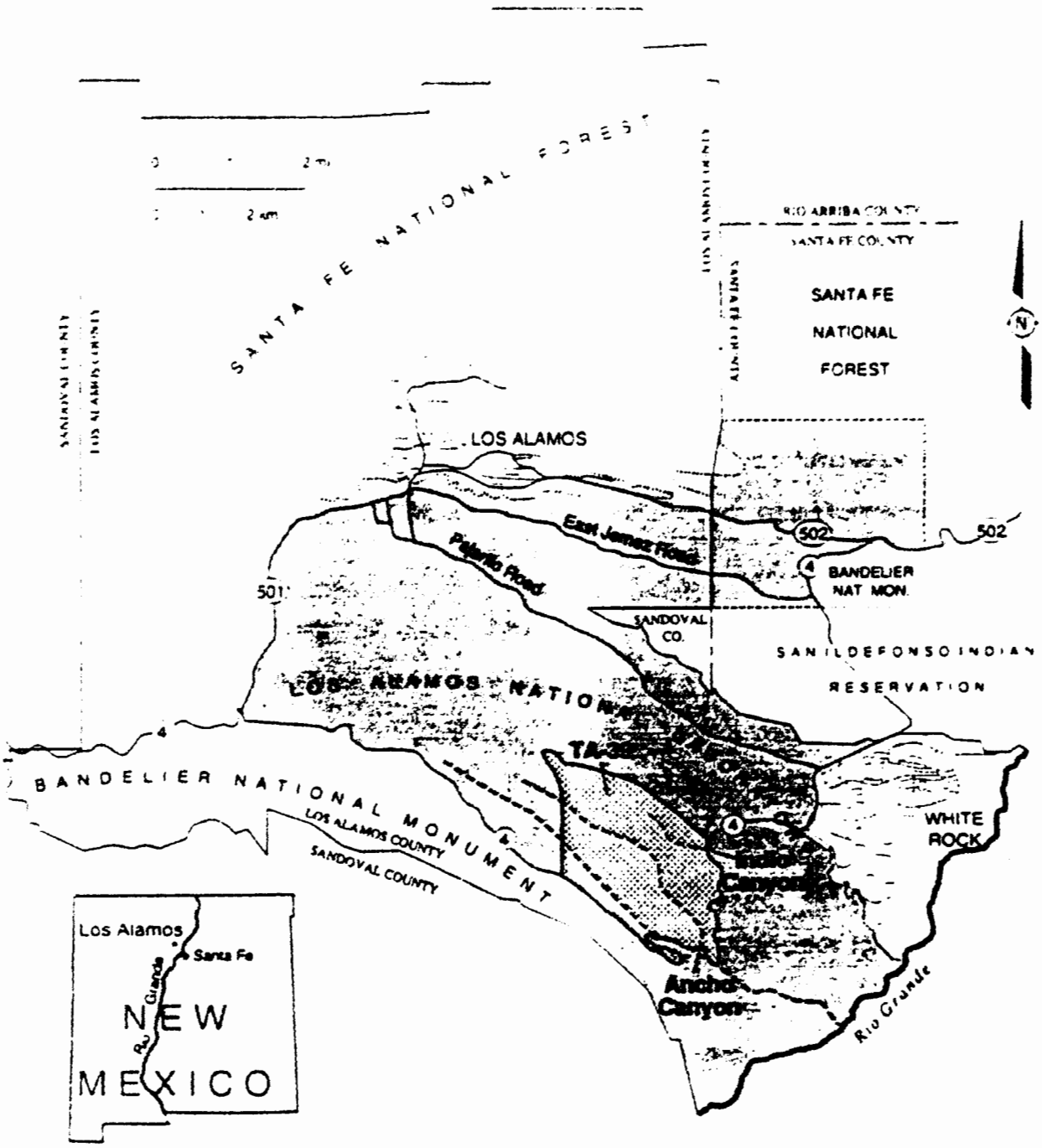
SANTA FE NATIONAL FOREST
RIO ARRIBA COUNTY
SANTA FE COUNTY
SANTA FE
NATIONAL
FOREST
N
LOS ALAMOS
East Jemez Road
Pajarito Road
502
502
4
BANDELIER
NAT MON.
501
SANDOVAL
CO.
SAN ILDEFONSO INDIAN
RESERVATION
LOS ALAMOS NATIONAL
4
BANDELIER NATIONAL MONUMENT
LOS ALAMOS COUNTY
SANDOVAL COUNTY
4
WHITE
ROCK
Canyon
Canyon
Rio Grande
Los Alamos
Santa Fe
Rio Grande
NEW
MEXICO

Fig. 1

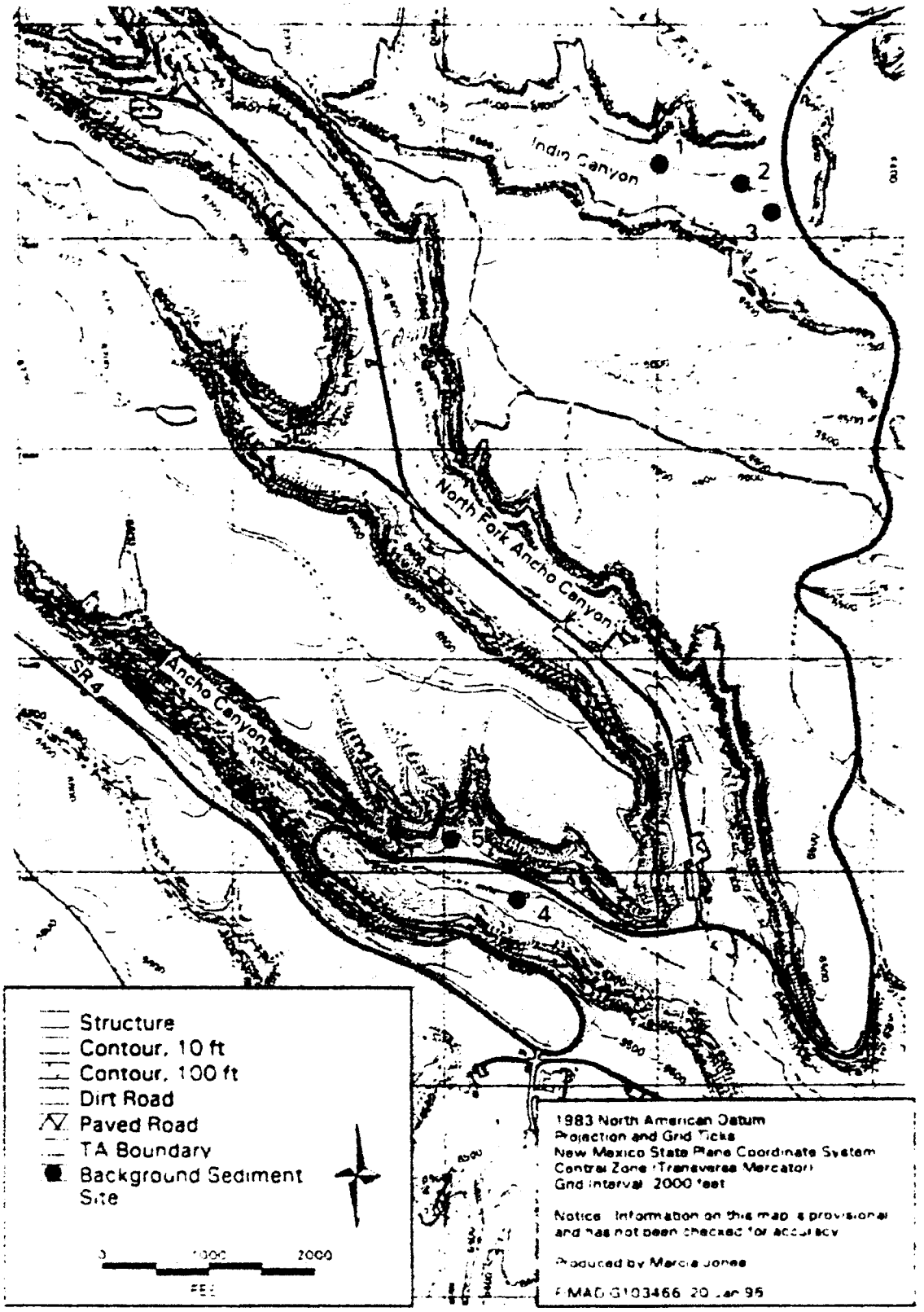
Indian Canyon
North Fork Ancho Canyon
Ancho Canyon
SR 4
1
2
3
4
5
Structure
Contour, 10 ft
Contour, 100 ft
Dirt Road
Paved Road
TA Boundary
Background Sediment Site
0
1000
2000
FEET
1983 North American Datum
Projection and Grid Ticks
New Mexico State Plane Coordinate System
Central Zone (Transverse Mercator)
Grid interval 2000 feet
Notice: Information on this map is provisional and has not been checked for accuracy
Produced by Marcia Jones
FMAD G103466 20 Jan 95

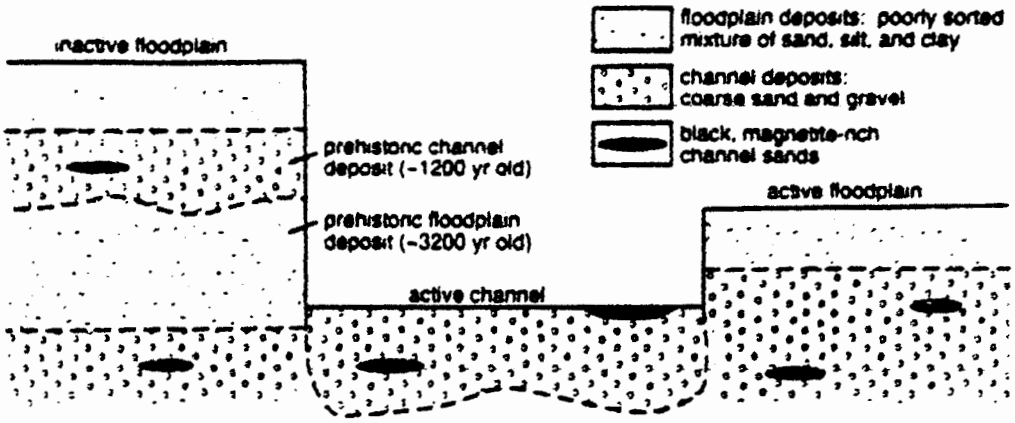
floodplain deposits: poorly sorted mixture of sand, silt, and clay
channel deposits: coarse sand and gravel
black, magnetite-rich channel sands
inactive floodplain
prehistoric channel deposit (~1200 yr old)
prehistoric floodplain deposit (~3200 yr old)
active channel
active floodplain

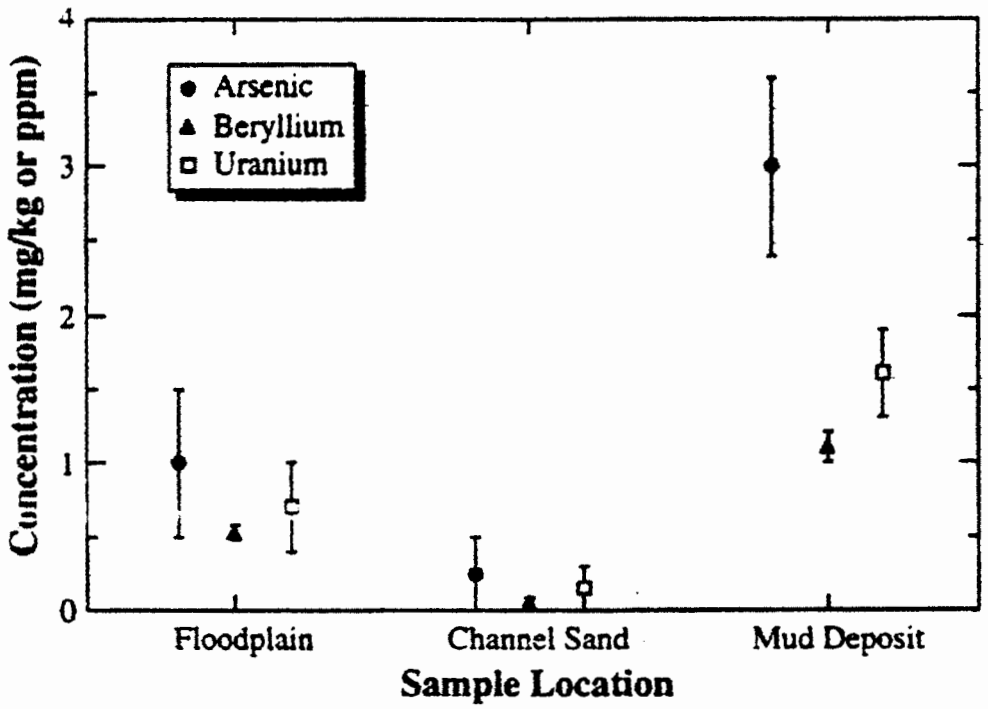
Arsenic
Beryllium
Uranium
Concentration (mg/kg or ppm)
0
1
2
3
4
Floodplain
Channel Sand
Mud Deposit
Sample Location

Fig. 4

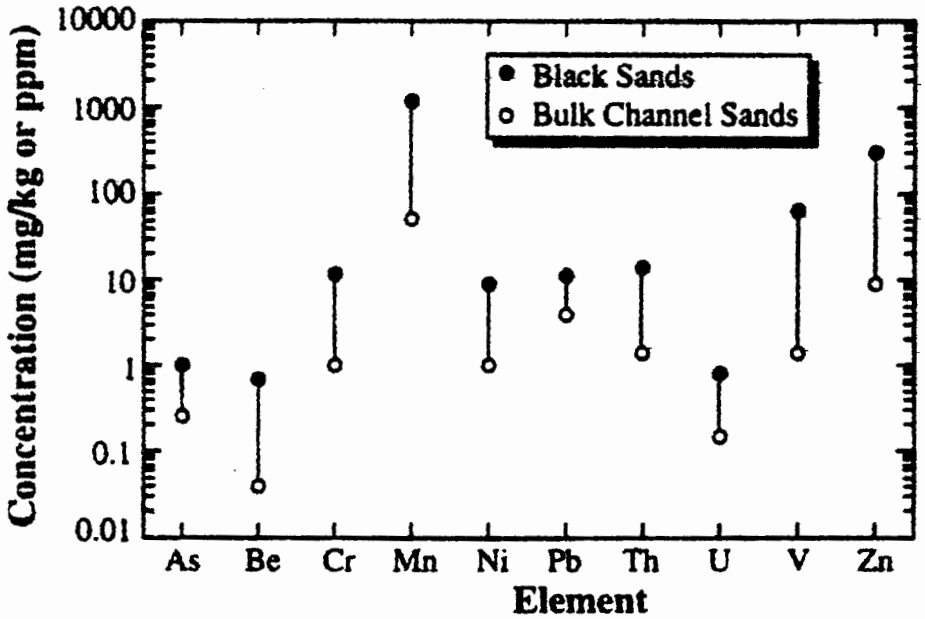
Black Sands
Bulk Channel Sands
Concentration (mg/kg or ppm)
10000
1000
100
10
1
0.1
0.01
As
Be
Cr
Mn
Ni
Pb
Th
U
V
Zn
Element

Fig. 5

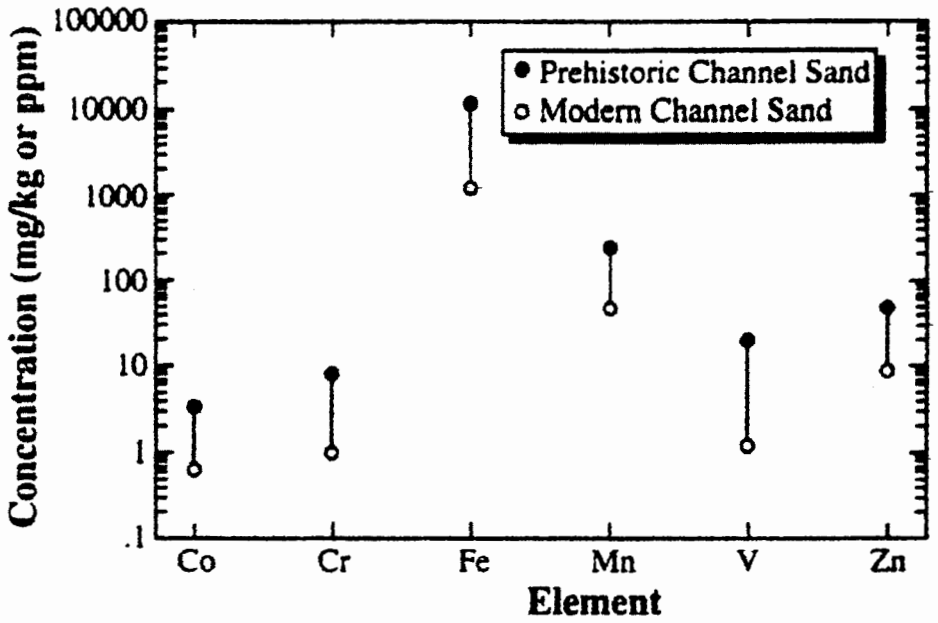
Concentration (mg/kg or ppm)
100000
10000
1000
100
10
1
.1
Prehistoric Channel Sand
Modern Channel Sand
Co
Cr
Fe
Mn
V
Zn
Element

**Fig. 6**

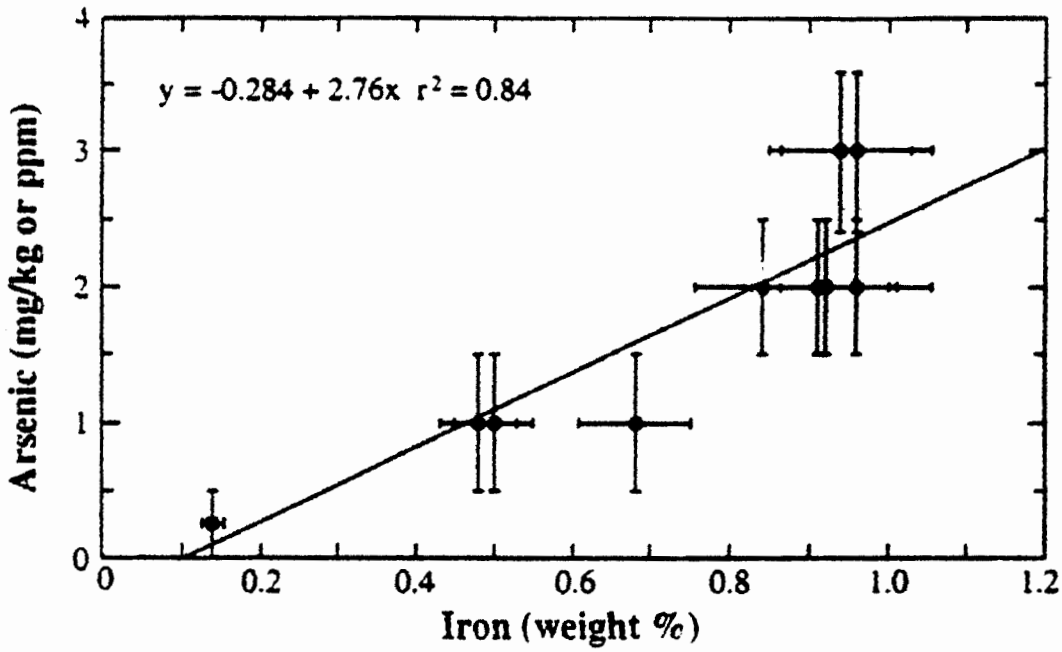
y = -0.284 + 2.76x r² = 0.84
Arsenic (mg/kg or ppm)
Iron (weight %)
0
1
2
3
4
0
0.2
0.4
0.6
0.8
1.0
1.2

Fig. 7

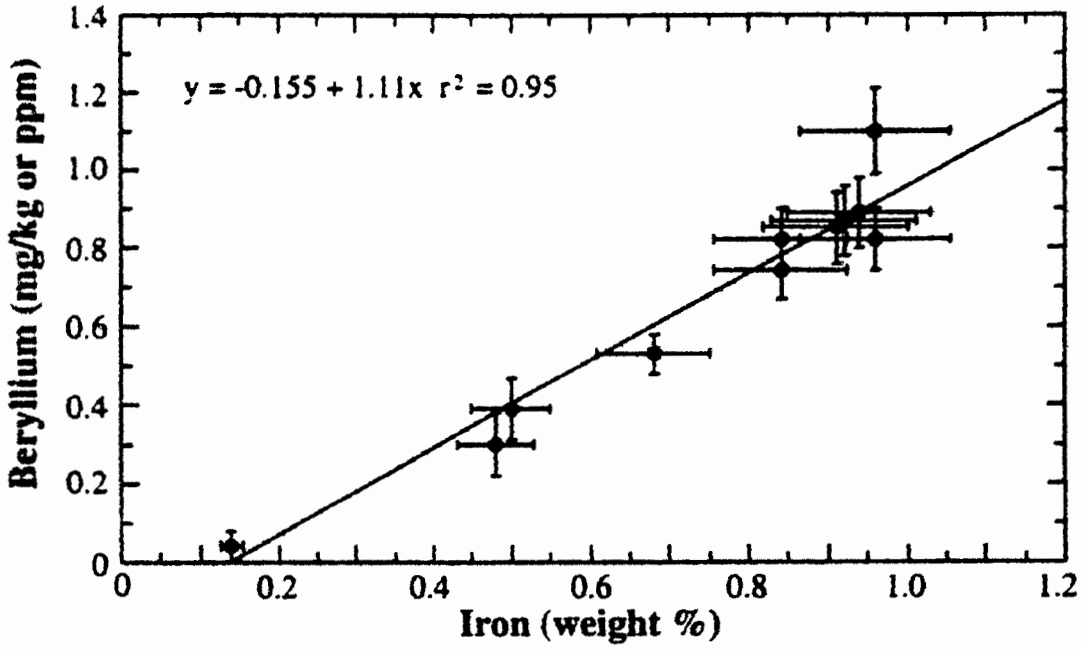
y = -0.155 + 1.11x r² = 0.95
Beryllium (mg/kg or ppm)
Iron (weight %)
0
0.2
0.4
0.6
0.8
1.0
1.2
1.4

Fig. 8

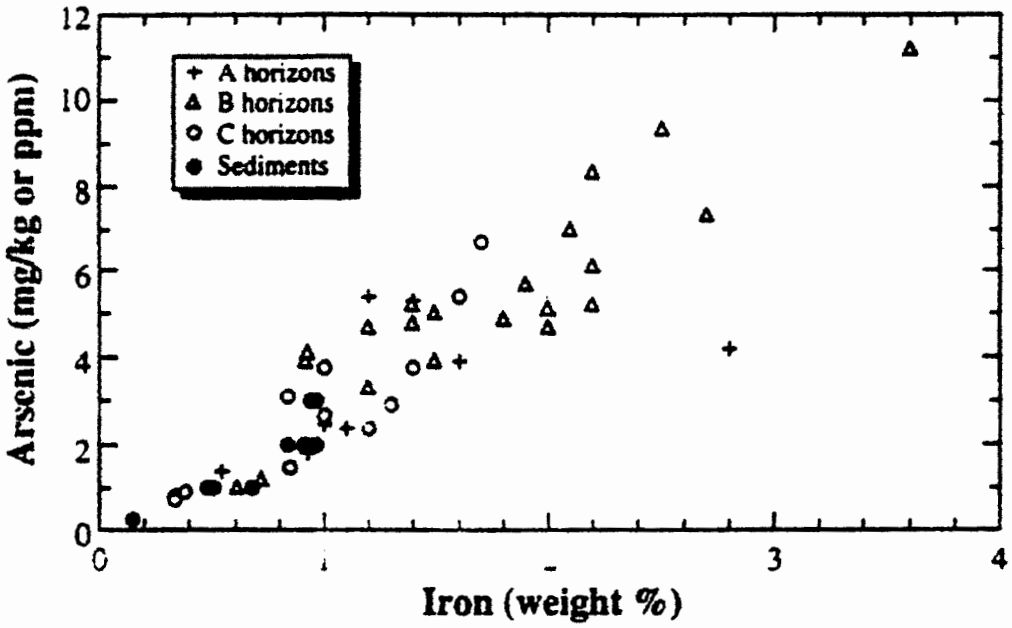
A horizons
B horizons
C horizons
Sediments
Arsenic (mg/kg or ppm)
Iron (weight %)
0
2
4
6
8
10
12
0
1
2
3
4

Fig. 9

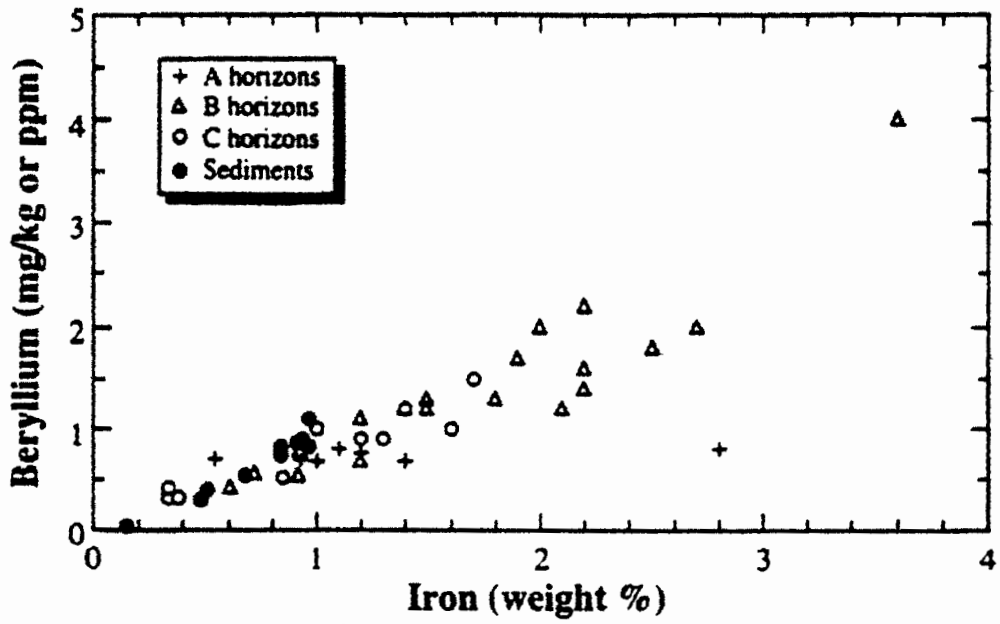
A horizons
B horizons
C horizons
Sediments
Beryllium (mg/kg or ppm)
Iron (weight %)
0
1
2
3
4
5

Fig. 9 10

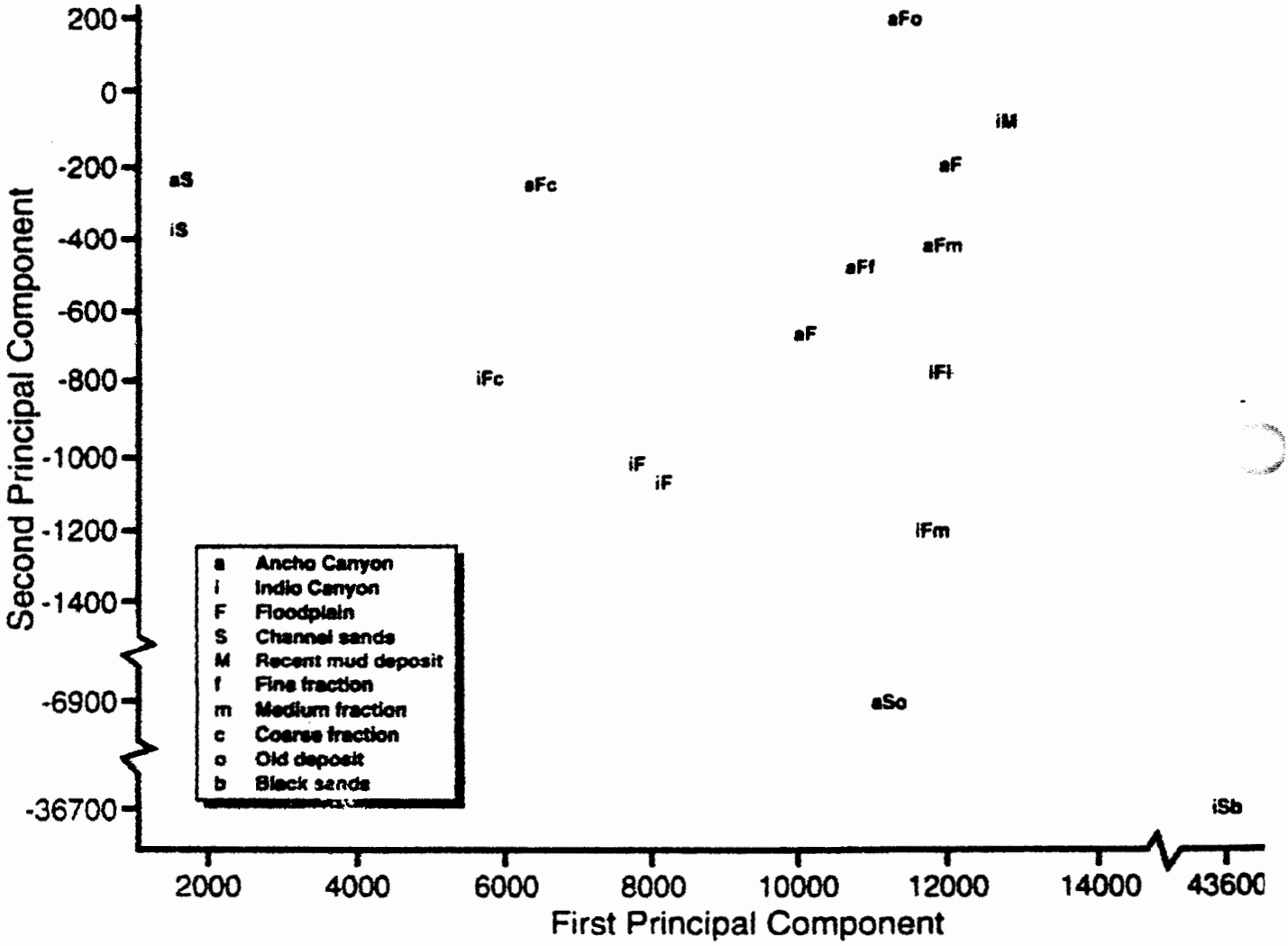
200
0
-200
-400
-600
-800
-1000
-1200
-1400
-6900
-36700
Second Principal Component
2000
4000
6000
8000
10000
12000
14000
43600
First Principal Component
aFo
iM
aF
aS
aFc
iS
aFm
aFf
aF
iFc
iFf
iF
iF
iFm
aSo
iSb
a Ancho Canyon
i Indio Canyon
F Floodplain
S Channel sands
M Recent mud deposit
f Fine fraction
m Medium fraction
c Coarse fraction
o Old deposit
b Black sands

Fig 11

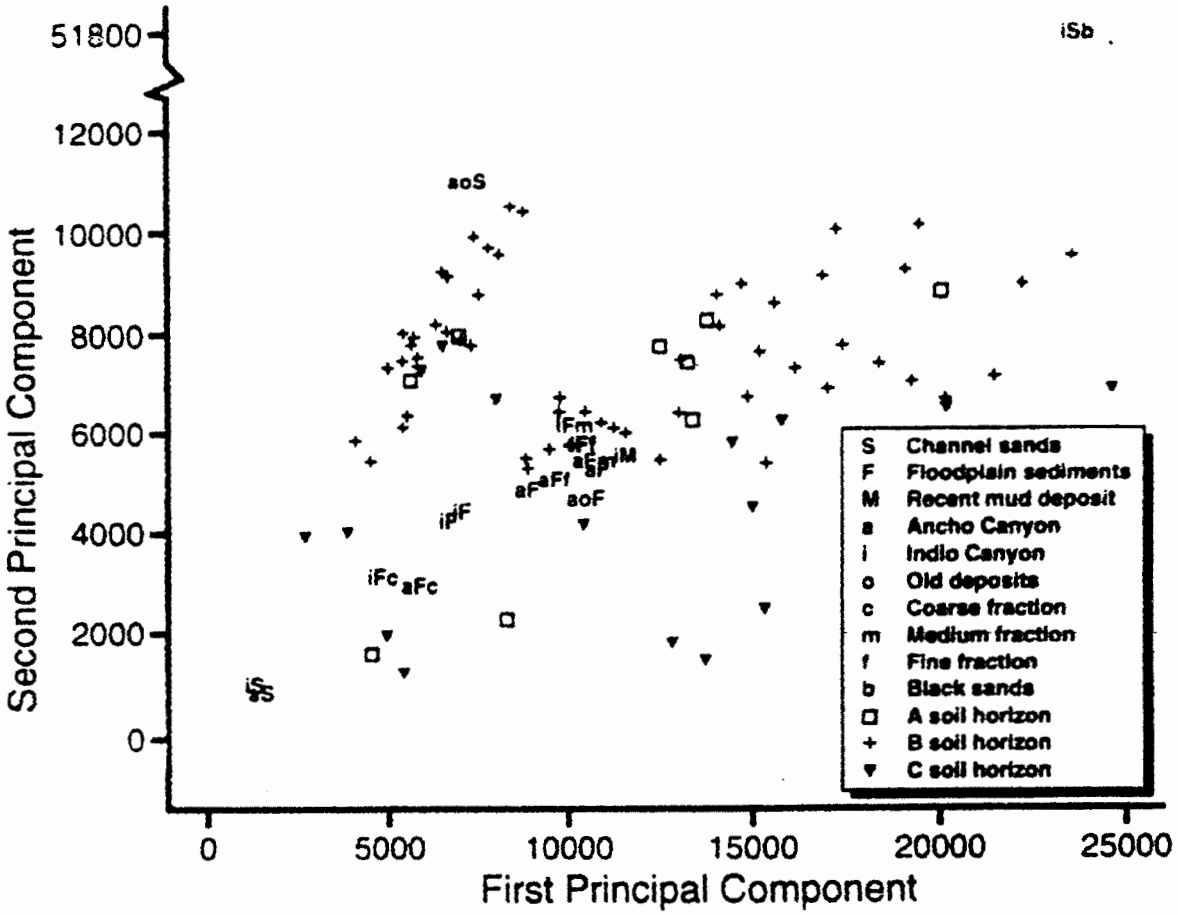
Second Principal Component
First Principal Component
51800
12000
10000
8000
6000
4000
2000
0
0
5000
10000
15000
20000
25000
iSb
aoS
iFm
4Ff
aFf
aF
aoF
iM
iF
iFc
aFc
iS
aS
S Channel sands
F Floodplain sediments
M Recent mud deposit
a Ancho Canyon
i Indio Canyon
o Old deposits
c Coarse fraction
m Medium fraction
f Fine fraction
b Black sands
A soil horizon
B soil horizon
C soil horizon

Fig 12

Table 1
Location of Sample Sites and Description of Samples, TA-39

| Sample Number | Sample Location * | Type of Deposit | Sample Depth | Particle Size | Notes |
|---|---|---|---|---|---|
| FS2220 | Indio Cyn, 6425' (1) | floodplain | 0-18" | < 2 mm (sand, silt, clay) | bulk sample, gravel removed |
| FS2221 | Indio Cyn, 6425' (1) | floodplain | 0-18" | < 0.075 mm (very fine sand, silt, clay) | sample split, sieved |
| FS2222 | Indio Cyn, 6425' (1) | floodplain | 0-18" | 0.25-0.075 mm (fine sand) | sample split, sieved |
| FS2223 | Indio Cyn, 6425' (1) | floodplain | 0-18" | < 2 mm (sand, silt, clay) | duplicate of FS 2220 |
| FS2224 | Indio Cyn, 6425' (1) | channel sands | 0-6" | < 2 mm (mainly coarse sand) | bulk sample, gravel removed |
| FS2225 | Indio Cyn, 6400' (2) | channel sands | 0-1" | < 2 mm (mainly fine sand) | black (magnetite) sands |
| FS2226 | Indio Cyn, 6387' (3) | mud in channel | 0-1" | < 2 mm (mainly fine sand, silt, clay) | mud deposits from recent flood |
| FS2227 | Ancho Cyn, 6228' (4) | old floodplain | 4.1-4.6' | < 2 mm (sand, silt, clay) | bulk sample, gravel removed |
| FS2228 | Ancho Cyn, 6228' (4) | old channel sands | 2.6-3.1' | < 2 mm (mainly coarse sand) | bulk sample, gravel removed |
| FS2229 | Ancho Cyn, 6295' (5) | floodplain | 8-16" | < 2 mm (sand, silt, clay) | bulk sample, gravel removed |
| FS2230 | Ancho Cyn, 6295' (5) | floodplain | 8-16" | < 0.075 mm (very fine sand, silt, clay) | sample split, sieved |
| FS2231 | Ancho Cyn, 6295' (5) | floodplain | 8-16" | 0.25-0.075 mm (fine sand) | sample split, sieved |
| FS2232 | Ancho Cyn, 6295' (5) | floodplain | 8-16" | < 2 mm (sand, silt, clay) | duplicate of FS 2229 |
| FS2233 | Ancho Cyn, 6295' (5) | channel sands | 0-6" | < 2 mm (mainly coarse sand) | bulk sample, gravel removed |
| FS2234 | Indio Cyn, 6425' (1) | floodplain | 0-18" | 0.25-2 mm (coarse+medium sand) | sample split, sieved |
| FS2235 | Ancho Cyn, 6295' (5) | floodplain | 8-16" | 0.25-2 mm (coarse+medium sand) | sample split, sieved |

* Elevations refer to approximate stream channel elevations at sample site, as obtained from FIMAD topographic maps. Numbers in () refer to site locations of Figure 2.

**Table 2. TA-39 Background Sediment Chemistry Data, $HNO_3$ Digestion ***

| Sample | Al (ppm) | Al (+/-) | As (ppm) | As (+/-) | Ba (ppm) | Ba (+/-) | Be (ppm) | Be (+/-) | Ca (ppm) | Ca (+/-) |
|---|---|---|---|---|---|---|---|---|---|---|
| FS2220 | 4600 | 460 | 1 | 0.5 | 53 | 5.3 | 0.53 | 0.05 | 1200 | 120 |
| FS2221 | 7300 | 730 | 3 | 0.60 | 99 | 9.90 | 0.89 | 0.09 | 1900 | 190 |
| FS2222 | 6900 | 690 | 2 | 0.50 | 77 | 7.70 | 0.82 | 0.08 | 1700 | 170 |
| FS2223 | 4400 | 440 | 2 | 0.50 | 54 | 5.40 | 0.56 | 0.06 | 1300 | 130 |
| FS2224 | 740 | 74 | <0.5 | | 8 | 0.80 | <0.08 | | 180 | 18 |
| FS2225 | 1400 | 140 | 1 | 0.50 | 14 | 1.40 | 0.70 | 0.08 | 990 | 99 |
| FS2226 | 8400 | 840 | 3 | 0.60 | 100 | 10 | 1.10 | 0.11 | 2600 | 260 |
| FS2227 | 7700 | 770 | 2 | 0.50 | 71 | 7.10 | 0.74 | 0.07 | 1500 | 150 |
| FS2228 | 2300 | 230 | 0.90 | 0.50 | 32 | 3 | 0.17 | 0.08 | 770 | 77 |
| FS2229 | 7800 | 780 | 2 | 0.50 | 90 | 9 | 0.85 | 0.09 | 2100 | 210 |
| FS2230 | 6800 | 680 | 2 | 0.50 | 90 | 9 | 0.82 | 0.08 | 2500 | 250 |
| FS2231 | 7600 | 760 | 3 | 0.60 | 95 | 9.50 | 0.87 | 0.09 | 2400 | 240 |
| FS2232 | 6200 | 620 | 2 | 0.50 | 75 | 7.50 | 0.67 | 0.08 | 1800 | 180 |
| FS2233 | 930 | 93 | <0.5 | | 8.30 | 0.83 | <0.08 | | 230 | 23 |
| FS2234 | 3200 | 320 | 1 | 0.50 | 37 | 3.70 | 0.30 | 0.08 | 960 | 96 |
| FS2235 | 4100 | 410 | 1 | 0.50 | 49 | 4.90 | 0.39 | 0.08 | 1100 | 110 |

| Sample | Co (ppm) | Co (+/-) | Cr (ppm) | Cr (+/-) | Cu (ppm) | Cu (+/-) | Fe (ppm) | Fe (+/-) | K (ppm) | K (+/-) | Mg (ppm) | Mg (+/-) |
|---|---|---|---|---|---|---|---|---|---|---|---|---|
| FS2220 | 2.2 | 0.5 | 3.5 | 0.5 | 3.5 | 0.5 | 6800 | 680 | 970 | 97 | 920 | 92 |
| FS2221 | 3.50 | 0.50 | 5.80 | 0.60 | 7.30 | 0.70 | 9400 | 940 | 1500 | 150 | 1500 | 150 |
| FS2222 | 3 | 0.50 | 4.70 | 0.50 | 5.60 | 0.60 | 9600 | 960 | 1400 | 140 | 1300 | 130 |
| FS2223 | 2.30 | 0.50 | 3.30 | 0.50 | 3.50 | 0.50 | 6500 | 650 | 990 | 99 | 870 | 87 |
| FS2224 | 0.60 | 0.50 | 1 | 0.50 | 0.80 | 0.50 | 1400 | 140 | 180 | 74 | 170 | 17 |
| FS2225 | 6 | 0.60 | 12 | 1.20 | 4.40 | 0.50 | 57000 | 5700 | 220 | 22 | 530 | 53 |
| FS2226 | 3.50 | 0.50 | 5.60 | 0.60 | 12 | 1.20 | 9600 | 960 | 1800 | 180 | 1700 | 170 |
| FS2227 | 2.70 | 0.50 | 5.20 | 0.50 | 4.30 | 0.50 | 8400 | 840 | 1600 | 160 | 1400 | 140 |
| FS2228 | 3.10 | 0.50 | 5.40 | 0.50 | 1.80 | 0.50 | 13000 | 1300 | 540 | 54 | 570 | 57 |
| FS2229 | 3.50 | 0.50 | 5.70 | 0.60 | 5.70 | 0.60 | 9100 | 910 | 1900 | 190 | 1500 | 150 |
| FS2230 | 3 | 0.50 | 5.90 | 0.60 | 7.50 | 0.80 | 8400 | 840 | 1900 | 190 | 1500 | 150 |
| FS2231 | 3.80 | 0.50 | 5.90 | 0.60 | 7.30 | 0.70 | 9200 | 920 | 2200 | 220 | 1600 | 160 |
| FS2232 | 3.20 | 0.50 | 4.70 | 0.50 | 4.80 | 0.50 | 8000 | 800 | 1600 | 160 | 1300 | 130 |
| FS2233 | 0.70 | 0.50 | 0.80 | 0.50 | 0.90 | 0.50 | 1400 | 140 | 200 | 20 | 200 | 20 |
| FS2234 | 1.50 | 0.50 | 2.20 | 0.50 | 2.70 | 0.50 | 4800 | 480 | 650 | 65 | 590 | 59 |
| FS2235 | 2 | 0.50 | 2.50 | 0.50 | 3 | 0.50 | 5000 | 500 | 1100 | 110 | 820 | 82 |

Table 2. TA-39 Background Sediment Chemistry Data, $HNO_3$ Digestion (continued)

| Sample | Mn (ppm) | Mn (+/-) | Na (ppm) | Na (+/-) | Ni (ppm) | Ni (+/-) | Pb (ppm) | Pb (+/-) | Sb (ppm) | Sb (+/-) |
|---|---|---|---|---|---|---|---|---|---|---|
| FS2220 | 240 | 24 | 120 | 14 | 4 | 2 | 5 | 4 | <5 | |
| FS2221 | 330 | 33 | 120 | 14 | 7 | 2 | 10 | 4 | <5 | |
| FS2222 | 350 | 35 | 120 | 14 | 5 | 2 | 10 | 4 | <5 | |
| FS2223 | 240 | 24 | 95 | 14 | 4 | 2 | 8 | 4 | <5 | |
| FS2224 | 53 | 5.30 | 46 | 14 | <2 | | 4 | 4 | <5 | |
| FS2225 | 1200 | 120 | 68 | 14 | 9 | 2 | 11 | 4 | <5 | |
| FS2226 | 380 | 38 | 190 | 19 | 6 | 2 | 16 | 4 | 5 | 5 |
| FS2227 | 220 | 22 | 150 | 15 | 4 | 2 | 7 | 4 | <5 | |
| FS2228 | 240 | 24 | 66 | 14 | 4 | 2 | 5 | 4 | <5 | |
| FS2229 | 330 | 33 | 100 | 14 | 6 | 2 | 10 | 4 | <5 | |
| FS2230 | 230 | 23 | 76 | 14 | 5 | 2 | 7 | 4 | <5 | |
| FS2231 | 300 | 30 | 110 | 14 | 7 | 2 | 9 | 4 | <5 | |
| FS2232 | 280 | 28 | 91 | 14 | 6 | 2 | 8 | 4 | <5 | |
| FS2233 | 46 | 4.60 | 34 | 14 | <2 | | <4 | | <5 | |
| FS2234 | 180 | 18 | 75 | 14 | 4 | 2 | 5 | 4 | <5 | |
| FS2235 | 190 | 19 | 80 | 14 | 4 | 2 | 6 | 4 | <5 | |

| Sample | Ta (ppm) | Ta (+/-) | Th (ppm) | Th (+/-) | Tl (ppm) | Tl (+/-) | U (ppm) | U (+/-) | V (ppm) | V (+/-) | Zn (ppm) | Zn (+/-) |
|---|---|---|---|---|---|---|---|---|---|---|---|---|
| FS2220 | <0.3 | | 5.2 | 0.4 | 0.5 | 0.3 | 0.7 | 0.3 | 7.2 | 0.7 | 31 | 3.1 |
| FS2221 | <0.3 | | 7.70 | 0.50 | <0.3 | | 0.90 | 0.30 | 12 | 1.20 | 38 | 3.80 |
| FS2222 | <0.3 | | 7.10 | 0.50 | <0.3 | | 1 | 0.30 | 10 | 1 | 44 | 4.40 |
| FS2223 | <0.3 | | 5.80 | 0.40 | <0.3 | | 0.90 | 0.30 | 7 | 0.70 | 31 | 3 |
| FS2224 | <0.3 | | 1.40 | 0.30 | <0.3 | | <0.3 | | 1.40 | 0.50 | 9 | 1 |
| FS2225 | <0.3 | | 14 | 1 | <0.3 | | 0.80 | 0.30 | 66 | 6.60 | 300 | 30 |
| FS2226 | <0.3 | | 6.60 | 0.50 | <0.3 | | 1.60 | 0.30 | 11 | 1.10 | 48 | 4.80 |
| FS2227 | <0.3 | | 5.80 | 0.40 | <0.3 | | 0.60 | 0.30 | 9 | 0.90 | 33 | 3 |
| FS2228 | <0.3 | | 2.20 | 0.30 | <0.3 | | <0.3 | | 20 | 2 | 47 | 5 |
| FS2229 | <0.3 | | 8 | 0.60 | <0.3 | | 0.70 | 0.30 | 11 | 1.10 | 39 | 4 |
| FS2230 | <0.3 | | 6.90 | 0.80 | <0.3 | | 0.60 | 0.30 | 13 | 1.30 | 32 | 3 |
| FS2231 | <0.3 | | 7.10 | 0.80 | <0.3 | | 0.60 | 0.30 | 12 | 1.20 | 37 | 3.70 |
| FS2232 | <0.3 | | 6 | 0.70 | <0.3 | | 0.60 | 0.30 | 9 | 0.90 | 34 | 3.40 |
| FS2233 | <0.3 | | 0.90 | 0.30 | <0.3 | | <0.3 | | 1 | 0.50 | 9 | 1 |
| FS2234 | <0.3 | | 3.60 | 0.40 | <0.3 | | 0.50 | 0.30 | 5 | 0.50 | 24 | 2 |
| FS2235 | <0.3 | | 4.30 | 0.50 | 1.50 | 0.30 | 0.40 | 0.30 | 5 | 0.50 | 24 | 2 |

* +/- is uncertainty reported by CST-3.

**Table 3. TA-39 Background Sediment Chemistry Data, HF Digestion ***

| Sample | Al (ppm) | Al (+/-) | As (ppm) | As (+/-) | Ba (ppm) | Ba (+/-) | Be (ppm) | Be (+/-) | Ca (ppm) | Ca (+/-) | Co (ppm) | Co (+/-) |
|---|---|---|---|---|---|---|---|---|---|---|---|---|
| FS2220 | 61000 | 6100 | 8.20 | 1.60 | 222 | 22 | 3.20 | 0.32 | 3800 | 380 | 2.30 | 0.50 |
| FS2221 | 57000 | 5700 | 5.30 | 1 | 370 | 37 | 3.80 | 0.38 | 4900 | 490 | 4 | 0.50 |
| FS2222 | 62000 | 6200 | 5.30 | 1 | 270 | 27 | 4.40 | 0.44 | 4300 | 430 | 3.80 | 0.50 |
| FS2223 | 61000 | 6100 | 6.30 | 1.30 | 240 | 24 | 3.50 | 0.35 | 4000 | 400 | 2.60 | 0.50 |
| FS2224 | 51000 | 5100 | 6.20 | 1.20 | 130 | 13 | 1.10 | 0.11 | 2000 | 200 | 0.70 | 0.50 |
| FS2225 | 11000 | 1100 | 4.80 | 1 | 32 | 3.20 | 1.60 | 0.16 | 3400 | 340 | < 0.5 | |
| FS2226 | 63000 | 6300 | 8.60 | 1.70 | 300 | 30 | 5.30 | 0.50 | 4900 | 490 | 3.40 | 0.50 |
| FS2227 | 69000 | 6900 | 10.40 | 2.10 | 340 | 34 | 4 | 0.40 | 6100 | 610 | 3.90 | 0.50 |
| FS2228 | 63000 | 6300 | 7.50 | 1.50 | 290 | 29 | 1.50 | 0.15 | 8100 | 810 | 7 | 0.70 |
| FS2229 | 60000 | 6000 | 8 | 1.60 | 330 | 33 | 3.60 | 0.36 | 4900 | 490 | 3.50 | 0.50 |
| FS2230 | 56000 | 5600 | 9.10 | 1.80 | 410 | 41 | 3.20 | 0.32 | 5800 | 580 | 3.80 | 0.50 |
| FS2231 | 59000 | 5900 | 5.90 | 1.20 | 380 | 38 | 3.60 | 0.36 | 5500 | 550 | 3.90 | 0.50 |
| FS2232 | 61000 | 6100 | 3.60 | 0.70 | 310 | 31 | 3.40 | 0.34 | 4700 | 470 | 3.30 | 0.50 |
| FS2233 | 48000 | 4800 | 2.10 | 0.40 | 120 | 12 | 0.91 | 0.09 | 1800 | 180 | 1 | 0.50 |
| FS2234 | 61000 | 6100 | 3 | 0.60 | 180 | 18 | 2.40 | 0.24 | 3400 | 340 | 1.50 | 0.50 |
| FS2235 | 59000 | 5900 | 2.50 | 0.50 | 210 | 21 | 2.90 | 0.29 | 3500 | 350 | 2 | 0.50 |

| Sample | Cr (ppm) | Cr (+/-) | Cu (ppm) | Cu (+/-) | Fe (ppm) | Fe (+/-) | K (ppm) | K (+/-) | Mg (ppm) | Mg (+/-) | Mn (ppm) | Mn (+/-) |
|---|---|---|---|---|---|---|---|---|---|---|---|---|
| FS2220 | 8.30 | 0.80 | 5.10 | 0.50 | 13000 | 1300 | 27000 | 2700 | 1700 | 170 | 420 | 42 |
| FS2221 | 18 | 1.80 | 12 | 1.20 | 17000 | 1700 | 23000 | 2300 | 2700 | 270 | 490 | 49 |
| FS2222 | 12 | 1.20 | 9.60 | 1 | 17000 | 1700 | 27000 | 2700 | 2500 | 250 | 580 | 58 |
| FS2223 | 9.90 | 1 | 6 | 0.60 | 14000 | 1400 | 29000 | 2900 | 1900 | 190 | 430 | 43 |
| FS2224 | 1.10 | 0.50 | 1 | 0.50 | 4900 | 490 | 26000 | 2600 | 470 | 47 | 180 | 18 |
| FS2225 | 83 | 8.30 | < 0.5 | | 110 | 11 | 3600 | 360 | 3000 | 300 | 13000 | 1300 |
| FS2226 | 14 | 1.40 | 15 | 1.50 | 16000 | 1600 | 26000 | 2600 | 2600 | 260 | 540 | 54 |
| FS2227 | 15 | 1.50 | 7.60 | 0.80 | 17000 | 1700 | 27000 | 2700 | 3300 | 330 | 450 | 45 |
| FS2228 | 23 | 2.30 | 2.60 | 0.50 | 52000 | 5200 | 25000 | 2500 | 2500 | 250 | 1300 | 130 |
| FS2229 | 15 | 1.50 | 8.70 | 0.90 | 16000 | 1600 | 26000 | 2600 | 2700 | 270 | 460 | 46 |
| FS2230 | 23 | 2.30 | 13 | 1.30 | 19000 | 1900 | 22000 | 2200 | 3100 | 310 | 420 | 42 |
| FS2231 | 17 | 1.70 | 13 | 1.30 | 18000 | 1800 | 24000 | 2400 | 3100 | 310 | 480 | 48 |
| FS2232 | 14 | 1.40 | 8.10 | 0.80 | 15000 | 1500 | 24000 | 2400 | 2500 | 250 | 430 | 43 |
| FS2233 | 2.50 | 0.50 | 1.20 | 0.50 | 4100 | 410 | 24000 | 2400 | 530 | 53 | 130 | 13 |
| FS2234 | 4.40 | 0.50 | 3.40 | 0.50 | 8500 | 850 | 25000 | 2500 | 1000 | 100 | 290 | 29 |
| FS2235 | 7.50 | 0.80 | 4.80 | 0.50 | 11000 | 1100 | 26000 | 2600 | 1600 | 160 | 330 | 33 |

Table 3. TA-39 Background Sediment Chemistry Data, HF Digestion (continued)

| Sample | Na (ppm) | Na (+/-) | Ni (ppm) | Ni (+/-) | Pb (ppm) | Pb (+/-) | Sb (ppm) | Sb (+/-) | Ta (ppm) | Ta (+/-) | Th (ppm) | Th (+/-) |
|---|---|---|---|---|---|---|---|---|---|---|---|---|
| FS2220 | 19000 | 1900 | 5 | 2 | 11 | 4 | < 5 | | 6 | 0.40 | 13 | 0.30 |
| FS2221 | 15000 | 1500 | 11 | 2 | 20 | 4 | < 5 | | 4.70 | 0.30 | 17 | 0.30 |
| FS2222 | 18000 | 1800 | 6 | 2 | 16 | 4 | < 5 | | 5.30 | 0.30 | 18 | 0.40 |
| FS2223 | 20000 | 2000 | 7 | 2 | 13 | 4 | < 5 | | 4.20 | 0.30 | 13 | 0.30 |
| FS2224 | 20000 | 2000 | < 2 | | < 4 | | < 5 | | 1.20 | 0.20 | 3.90 | 0.20 |
| FS2225 | 2700 | 270 | 47 | 5 | 50 | 5 | 14 | 5 | 15 | 0.90 | 130 | 4 |
| FS2226 | 18000 | 1800 | 7 | 2 | 27 | 4 | < 5 | | 5.70 | 0.30 | 18 | 0.40 |
| FS2227 | 18000 | 1800 | 8 | 2 | 14 | 4 | < 5 | | 4.40 | 0.40 | 15 | 0.60 |
| FS2228 | 20000 | 2000 | 14 | 2 | < 4 | | < 5 | | 2.60 | 0.30 | 9.40 | 0.40 |
| FS2229 | 16000 | 1600 | 8 | 2 | 12 | 4 | < 5 | | 4.30 | 0.40 | 15 | 0.60 |
| FS2230 | 14000 | 1400 | 10 | 2 | 13 | 4 | < 5 | | 4 | 0.40 | 16 | 0.60 |
| FS2231 | 14000 | 1400 | 8 | 2 | 13 | 4 | < 5 | | 4.40 | 0.40 | 15 | 0.60 |
| FS2232 | 16000 | 1600 | 14 | 2 | 13 | 4 | < 5 | | 4.60 | 0.50 | 15 | 0.60 |
| FS2233 | 18000 | 1800 | < 2 | | 4 | 4 | < 5 | | 0.90 | 0.20 | 3.30 | 0.20 |
| FS2234 | 21000 | 2100 | 2 | 2 | 8 | 4 | < 5 | | 3 | 0.30 | 8.80 | 0.40 |
| FS2235 | 19000 | 1900 | 5 | 2 | 10 | 4 | < 5 | | 3.20 | 0.30 | 10 | 0.40 |

| Sample | Tl (ppm) | Tl (+/-) | U (ppm) | U (+/-) | V (ppm) | V (+/-) | Zn (ppm) | Zn (+/-) |
|---|---|---|---|---|---|---|---|---|
| FS2220 | 0.50 | 0.20 | 3.90 | 0.20 | 16 | 1.60 | 64 | 6.40 |
| FS2221 | 0.70 | 0.20 | 5.70 | 0.30 | 33 | 3.30 | 70 | 7 |
| FS2222 | 0.70 | 0.20 | 5.60 | 0.30 | 25 | 2.50 | 88 | 8.80 |
| FS2223 | 0.50 | 0.20 | 4 | 0.20 | 19 | 1.90 | 66 | 6.60 |
| FS2224 | 0.20 | 0.20 | 1.10 | 0.20 | 2.70 | 0.50 | 25 | 2.50 |
| FS2225 | 0.30 | 0.20 | 4 | 0.20 | 450 | 45 | 2500 | 250 |
| FS2226 | 0.90 | 0.30 | 7.20 | 0.40 | 25 | 2.50 | 89 | 8.90 |
| FS2227 | 0.80 | 0.20 | 4.70 | 0.40 | 27 | 2.70 | 72 | 7.20 |
| FS2228 | 0.40 | 0.20 | 1.50 | 0.20 | 84 | 8.40 | 210 | 21 |
| FS2229 | 0.80 | 0.20 | 4.30 | 0.30 | 27 | 2.70 | 69 | 7 |
| FS2230 | 0.80 | 0.20 | 4.90 | 0.40 | 41 | 4.10 | 68 | 6.80 |
| FS2231 | 0.80 | 0.20 | 4.30 | 0.30 | 33 | 3.30 | 73 | 7.30 |
| FS2232 | 0.80 | 0.20 | 4.30 | 0.30 | 26 | 2.60 | 65 | 6.50 |
| FS2233 | 0.30 | 0.20 | 0.70 | 0.20 | 4 | 0.50 | 34 | 3.40 |
| FS2234 | 0.50 | 0.20 | 2.50 | 0.20 | 9 | 0.90 | 43 | 4.30 |
| FS2235 | 0.60 | 0.20 | 3 | 0.20 | 14 | 1.40 | 52 | 5.20 |

* +/- is uncertainty reported by CST-3.

**Table 4**
**TA-39 Background Sediment Chemistry Data,**
**Deionized Water Leachate ***

| Sample | Cl (ppm) | Cl (+/-) | $SO_4$ (ppm) | $SO_4$ (+/-) |
|---|---|---|---|---|
| FS2220 | <2.5 | | <5 | |
| FS2221 | <2.5 | | 10 | 5 |
| FS2222 | <2.5 | | 5.9 | 5 |
| FS2223 | <2.5 | | <5 | |
| FS2224 | <2.5 | | <5 | |
| FS2225 | <2.5 | | <5 | |
| FS2226 | <2.5 | | <5 | |
| FS2227 | 8.4 | 2.5 | 35 | 5 |
| FS2228 | 10.3 | 2.5 | 26.5 | 5 |
| FS2229 | <2.5 | | <5 | |
| FS2230 | <2.5 | | <5 | |
| FS2231 | <2.5 | | <5 | |
| FS2232 | <2.5 | | <5 | |
| FS2233 | <2.5 | | <5 | |
| FS2234 | <2.5 | | <5 | |
| FS2235 | <2.5 | | <5 | |

* +/- is uncertainty reported by CST-3.

**Table 5**
**Summary of Background Sediment Analyses, TA-39, $HNO_3$ and Deionized Water Digestion**

| Element | Coarse Channel Sands, Average (ppm) * | Bulk Floodplain Deposit, Average (ppm) ** | Minimum Value in Data Set (ppm) *** | Maximum Value in Data Set (ppm) *** |
|---|---|---|---|---|
| Al | 835 ± 134 | 5750 ± 1768 | 740 a | 8400 c |
| As | < 0.5 | 1.8 ± 0.4 | < 0.5 a | 3 c, e, f |
| Ba | 8.2 ± 0.2 | 68 ± 21 | 8 a | 100 c |
| Be | < 0.08 | 0.65 ± 0.15 | < 0.08 a | 1.1 c |
| Ca | 205 ± 35 | 1600 ± 495 | 180 a | 2600 c |
| Cl | < 2.5 | < 2.5 | < 2.5 | 10.3 i |
| Co | 0.65 ± 0.07 | 2.8 ± 0.8 | 0.6 a | 3.8 f |
| Cr | 0.9 ± 0.14 | 4.3 ± 1.3 | 0.8 a | 5.9 e, f |
| Cu | 0.85 ± 0.07 | 4.4 ± 1.2 | 0.8 a | 7.3 e |
| Fe | 1400 ± 140 | 7650 ± 1273 | 1400 a | 57000 d |
| K | 190 ± 14 | 1365 ± 544 | 180 a | 2200 f |
| Mg | 185 ± 21 | 1148 ± 357 | 170 a | 1700 c |
| Mn | 50 ± 5 | 273 ± 46 | 46 a | 1200 d |
| Na | 40 ± 8 | 102 ± 8 | 34 a | 190 c |
| Ni | < 2 | 5 ± 1.4 | < 2 a | 9 d |
| Pb | < 4 | 7.8 ± 1.8 | < 4 a | 16 c |
| Sb | < 5 | < 5 | < 5 | 5 d |
| SO4 | < 5 | < 5 | < 5 | 26.5 i |
| Ta | < 0.3 | < 0.3 | < 0.3 | < 0.3 |
| Th | 1.2 ± 0.4 | 6.3 ± 1.1 | 0.9 a | 14 d |
| Tl | < 0.3 | < 0.3 | < 0.3 | 1.5 g |
| U | < 0.3 | 0.7 ± 0.1 | < 0.3 a | 1.6 c |
| V | 1.2 ± 0.3 | 8.6 ± 2.1 | 1 a | 66 d |
| Zn | 9 ± 1 | 34 ± 4 | 9 a | 300 d |

* Samples FS2224 and FS2233. Uncertainty is 1σ.
** Samples FS2220, FS2223 (duplicate), FS2229, and FS2232 (duplicate). Uncertainty is 1σ.
*** a = coarse channel sands; b = bulk floodplain deposit; c= mud deposit; d = black sands; e = very fine sand to clay separate of floodplain sample; f = fine sand separate of floodplain deposit; g = coarse to medium sand separate of floodplain deposit; h = 3000 year old floodplain deposit; i = 1200 year old coarse channel sand.

**Table 6**
**Summary of Background Sediment Analyses, TA-39, HF Digestion**

| Element | Coarse Channel Sands, Average (ppm) * | Bulk Floodplain Deposit, Average (ppm) ** | Minimum Value in Data Set (ppm) *** | Maximum Value in Data Set (ppm) *** |
|---|---|---|---|---|
| Al | 49500 ± 2121 | 60750 ± 354 | 11000 d | 69000 h |
| As | 4.2 ± 2.9 | 6.8 ± 0.6 | 2.1 a | 10.4 h |
| Ba | 125 ± 7 | 276 ± 63 | 32 d | 410 e |
| Be | 1.0 ± 0.1 | 3.4 ± 0.1 | 0.91 a | 5.3 c |
| Ca | 1900 ± 141 | 4350 ± 636 | 1800 a | 8100 i |
| Co | 0.9± 0.2 | 3.0 ± 0.7 | < 0.5 d | 7 i |
| Cr | 1.8 ± 1.0 | 11.8 ± 3.8 | 1.1 a | 83 d |
| Cu | 1.1 ± 0.1 | 7.0 ± 2.0 | < 0.5 d | 13 e, f |
| Fe | 4500 ± 566 | 14500 ± 1414 | 4100 a | **** |
| K | 25000 ± 1414 | 26550 ± 2121 | 3600 a | 29000 b |
| Mg | 500 ± 42 | 2200 ± 566 | 470 a | 3300 h |
| Mn | 155 ± 35 | 435 ± 14 | 130 a | 13000 d |
| Na | 19000 ± 1414 | 17750 ± 2475 | 2700 d | 21000 g |
| Ni | < 2 | 8.5 ± 3.5 | < 2 a | 47 d |
| Pb | < 4 | 12 ± 0.4 | < 4 a, i | 27 c |
| Sb | < 5 | < 5 | < 5 | 14 d |
| Ta | 1.1 ± 0.2 | 4.8 ± 0.5 | 0.9 a | 6 b |
| Th | 3.6 ± 0.4 | 14 ± 1.4 | 3.3 a | 130 d |
| Tl | 0.3 ± 0.1 | 0.7 ± 0.2 | 0.2 a | 0.9 c |
| U | 0.9 ± 0.3 | 4.1 ± 0.3 | 0.7 a | 7.2 c |
| V | 3.4 ± 0.9 | 22 ± 6 | 2.7 a | 450 d |
| Zn | 30 ± 6 | 66 ± 1 | 25 a | 2500 d |

* Samples FS2224 and FS2233. Uncertainty is 1σ.
** Samples FS2220, FS2223 (duplicate), FS2229, and FS2232 (duplicate). Uncertainty is 1σ.
*** a = coarse channel sands; b = bulk floodplain deposit; c= mud deposit; d = black sands; e = very fine sand to clay separate of floodplain sample; f = fine sand separate of floodplain deposit; g = coarse to medium sand separate of floodplain deposit; h = 3000 year old floodplain deposit; i = 1200 year old coarse channel sand.
**** Highest Fe value should be in magnetite-rich black sand, but reported value believed to be in error because it is less than the Fe in the other samples and less than the Fe in the black sand sample from the $HNO_3$ digestion.

**Table 7**
**Summary of Different Size Fractions, TA-39, $HNO_3$ and Deionized Water Digestion**

| Element | Coarse Channel Sands, Average (ppm) * | Coarse and Medium Sand, Average (ppm) ** | Fine Sand, Average (ppm) *** | Very Fine Sand, Silt, Clay, Average (ppm) **** |
|---|---|---|---|---|
| Al | 835 ± 134 | 3650 ± 636 | 7250 ± 495 | 7050 ± 354 |
| As | < 0.5 | 1 ± 0.5 | 2.5 ± 0.7 | 2.5 ± 0.7 |
| Ba | 8.2 ± 0.2 | 43 ± 8 | 86 ± 13 | 95 ± 6 |
| Be | < 0.08 | 0.35± 0.06 | 0.85 ± 0.04 | 0.86 ± 0.05 |
| Ca | 205 ± 35 | 1030 ± 99 | 2050 ± 495 | 2200 ± 424 |
| Cl | < 2.5 | < 2.5 | < 2.5 | < 2.5 |
| Co | 0.65 ± 0.07 | 1.8 ± 0.4 | 3.4 ± 0.6 | 3.3 ± 0.4 |
| Cr | 0.9 ± 0.14 | 2.4 ± 0.2 | 5.3 ± 0.9 | 5.9 ± 0.1 |
| Cu | 0.85 ± 0.07 | 2.9 ± 0.2 | 6.5 ± 1.2 | 7.4 ± 0.1 |
| Fe | 1400 ± 140 | 4900 ± 141 | 9400 ± 283 | 8900 ± 707 |
| K | 190 ± 14 | 875 ± 318 | 1800 ± 566 | 1700 ± 283 |
| Mg | 185 ± 21 | 705 ± 163 | 1450 ± 212 | 1500 ± 150 |
| Mn | 50 ± 5 | 185 ± 7 | 325 ± 35 | 280 ± 71 |
| Na | 40 ± 8 | 78 ± 4 | 115 ± 7 | 98 ± 31 |
| Ni | < 2 | 4 ± 2 | 6.0 ± 1.4 | 6.0 ± 1.4 |
| Pb | < 4 | 5.5 ± 0.7 | 9.5 ± 0.7 | 8.5 ± 2.1 |
| Sb | < 5 | < 5 | < 5 | < 5 |
| SO4 | < 5 | < 5 | < 5.5 | < 7.5 |
| Ta | < 0.3 | < 0.3 | < 0.3 | < 0.3 |
| Th | 1.2 ± 0.4 | 4.0 ± 0.5 | 7.1 ± 0.5 | 7.3 ± 0.6 |
| Tl | < 0.3 | < 0.9 | < 0.3 | < 0.3 |
| U | < 0.3 | 0.45 ± 0.07 | 0.80 ± 0.28 | 0.75 ± 0.21 |
| V | 1.2 ± 0.3 | 5 ± 0.5 | 11 ± 1 | 13 ± 1 |
| Zn | 9 ± 1 | 24 ± 2 | 41 ± 5 | 35 ± 4 |

* Samples FS2224 and FS2233: bulk channel samples, dominated by coarse sand. Uncertainties are 1σ.
** Samples FS2234 and FS2235: 0.25-2.0 mm fraction. Uncertainties are 1σ.
*** Samples FS2222 and FS2231: 0.75-0.25 mm fraction. Uncertainties are 1σ.
*** Samples FS2221 and FS2230: <0.75 mm fraction. Uncertainties are 1σ.

**Table 8**
**Summary of Different Size Fractions, TA-39, HF Digestion**

| Element | Coarse Channel Sands, Average (ppm) * | Coarse and Medium Sand, Average (ppm) ** | Fine Sand, Average (ppm) *** | Very Fine Sand, Silt, Clay, Average (ppm) **** |
|---|---|---|---|---|
| Al | 49500 ± 2121 | 60000 ± 1414 | 60500 ± 2121 | 56500 ± 707 |
| As | 4.2 ± 2.9 | 2.8 ± 0.4 | 5.6 ± 0.4 | 7.2 ± 2.7 |
| Ba | 125 ± 7 | 195 ± 21 | 325 ± 78 | 390 ± 28 |
| Be | 1.0 ± 0.1 | 2.7 ± 0.4 | 4.0 ± 0.6 | 3.5 ± 0.4 |
| Ca | 1900 ± 141 | 3450 ± 71 | 4900 ± 849 | 5350 ± 636 |
| Co | 0.9± 0.2 | 1.8 ± 0.4 | 3.9 ± 0.1 | 3.9 ± 0.1 |
| Cr | 1.8 ± 1.0 | 6.0 ± 2.2 | 15 ± 4 | 21 ± 4 |
| Cu | 1.1 ± 0.1 | 4.1 ± 1.0 | 11 ± 2 | 13 ± 1 |
| Fe | 4500 ± 566 | 9750 ± 1768 | 17500 ± 707 | 18000 ± 1414 |
| K | 25000 ± 1414 | 25500 ± 707 | 25500 ± 2121 | 22500 ± 707 |
| Mg | 500 ± 42 | 1300 ± 424 | 2800 ± 424 | 2900 ± 283 |
| Mn | 155 ± 35 | 295 ± 50 | 530 ± 71 | 455 ± 50 |
| Na | 19000 ± 1414 | 20000 ± 1414 | 16000 ± 2828 | 14500 ± 707 |
| Ni | < 2 | 3.5 ± 2.1 | 7.0 ± 1.4 | 11 ± 1 |
| Pb | < 4 | 9.0 ± 1.4 | 15 ± 2 | 17 ± 5 |
| Sb | < 5 | < 5 | < 5 | < 5 |
| Ta | 1.1 ± 0.2 | 3.1 ± 0.1 | 4.9 ± 0.6 | 4.4 ± 0.5 |
| Th | 3.6 ± 0.4 | 9.4 ± 0.9 | 17 ± 2 | 17 ± 1 |
| Tl | 0.3 ± 0.1 | 0.6 ± 0.1 | 0.8 ± 0.1 | 0.8 ± 0.1 |
| U | 0.9 ± 0.3 | 2.8 ± 0.4 | 5.0 ± 0.9 | 5.3 ± 0.6 |
| V | 3.4 ± 0.9 | 12 ± 4 | 29 ± 6 | 37 ± 6 |
| Zn | 30 ± 6 | 48 ± 6 | 81 ± 11 | 69 ± 1 |

* Samples FS2224 and FS2233: bulk channel samples, dominated by coarse sand. Uncertainties are 1σ.
** Samples FS2234 and FS2235: 0.25-2.0 mm fraction. Uncertainties are 1σ.
*** Samples FS2222 and FS2231: 0.75-0.25 mm fraction. Uncertainties are 1σ.
*** Samples FS2221 and FS2230: <0.75 mm fraction. Uncertainties are 1σ

## Table 9
## Comparison of Modern and Old Deposits, TA-39, $HNO_3$ and Deionized Water Digestion

| Element | Coarse Channel Sands, Average (ppm) * | Old Channel Sands (ppm) ** | Bulk Floodplain Deposit, Average (ppm) *** | Old Floodplain Deposits (ppm) **** |
|---|---|---|---|---|
| Al | 835 ± 134 | 2300 a | 5750 ± 1768 | 7700 |
| As | < 0.5 | 0.9 | 1.8 ± 0.4 | 2 |
| Ba | 8.2 ± 0.2 | 32 a | 68 ± 21 | 71 |
| Be | < 0.08 | 0.17 a | 0.65 ± 0.15 | 0.74 |
| Ca | 205 ± 35 | 770 a | 1600 ± 495 | 1500 |
| Cl | < 2.5 | 10.3 b, c | < 2.5 | 8.4 b |
| Co | 0.65 ± 0.07 | 3.1 b | 2.8 ± 0.8 | 2.7 |
| Cr | 0.9 ± 0.14 | 5.4 b | 4.3 ± 1.3 | 5.2 |
| Cu | 0.85 ± 0.07 | 1.8 a | 4.4 ± 1.2 | 4.3 |
| Fe | 1400 ± 140 | 13000 b | 7650 ± 1273 | 8400 |
| K | 190 ± 14 | 540 a | 1365 ± 544 | 1600 |
| Mg | 185 ± 21 | 570 a | 1148 ± 357 | 1400 |
| Mn | 50 ± 5 | 240 b | 273 ± 46 | 220 |
| Na | 40 ± 8 | 66 | 102 ± 8 | 150 b |
| Ni | < 2 | 4 | 5 ± 1.4 | 4 |
| Pb | < 4 | 7 | 7.8 ± 1.8 | 7 |
| Sb | < 5 | < 5 | < 5 | < 5 |
| SO4 | < 5 | 26.5 b | < 5 | 35 b, c |
| Ta | < 0.3 | < 0.3 | < 0.3 | < 0.3 |
| Th | 1.2 ± 0.4 | 2.2 a | 6.3 ± 1.1 | 5.8 |
| Tl | < 0.3 | < 0.3 | < 0.3 | < 0.3 |
| U | < 0.3 | < 0.3 | 0.7 ± 0.1 | 0.6 |
| V | 1.2 ± 0.3 | 20 b | 8.6 ± 2.1 | 9 |
| Zn | 9 ± 1 | 47 b | 34 ± 4 | 33 |

* Samples FS2224 and FS2233. Uncertainties are 1σ.

** Sample FS2228; a = beyond range of modern channel sands, but within range of medium to coarse sand separate of banks; b = beyond range of medium to coarse sand separate of floodplain deposits; c = maximum value from this data set.

*** Samples FS2220, FS2223 (duplicate), FS2229, and FS2232 (duplicate). Uncertainties are 1σ.

**** Sample FS2227; a = beyond range of modern bulk floodplain deposits, but within range of fine sand to clay separates of floodplain deposits; b = beyond range of fine sand to clay separates of floodplain deposits; c = maximum value from this data set.

**Table 10**
**Comparison of Modern and Old Deposits, TA-39, HF Digestion**

| Element | Coarse Channel Sands, Average (ppm) * | Old Channel Sands (ppm) ** | Bulk Floodplain Deposit, Average (ppm) *** | Old Floodplain Deposits (ppm) **** |
|---|---|---|---|---|
| Al | 49500 ± 2121 | 63000 a | 60750 ± 354 | 69000 c |
| As | 4.2 ± 2.9 | 7.5 | 6.8 ± 0.6 | 10.4 a |
| Ba | 125 ± 7 | 290 b | 276 ± 63 | 340 |
| Be | 1.0 ± 0.1 | 1.5 a | 3.4 ± 0.1 | 4 |
| Ca | 1900 ± 141 | 8100 b, c | 4350 ± 636 | 6100 a |
| Co | 0.9± 0.2 | 7 b, c | 3.0 ± 0.7 | 3.9 |
| Cr | 1.8 ± 1.0 | 23 b | 11.8 ± 3.8 | 15 |
| Cu | 1.1 ± 0.1 | 2.6 a | 7.0 ± 2.0 | 7.6 |
| Fe | 4500 ± 566 | 52000 b, c? | 14500 ± 1414 | 17000 |
| K | 25000 ± 1414 | 25000 | 26550 ± 2121 | 27000 |
| Mg | 500 ± 42 | 2500 b | 2200 ± 566 | 3300 |
| Mn | 155 ± 35 | 1300 b | 435 ± 14 | 450 |
| Na | 19000 ± 1414 | 20000 | 17750 ± 2475 | 18000 |
| Ni | < 2 | 14 b | 8.5 ± 3.5 | 8 |
| Pb | < 4 | < 4 | 12 ± 0.4 | 14 |
| Sb | < 5 | < 5 | < 5 | < 5 |
| Ta | 1.1 ± 0.2 | 2.6 a | 4.8 ± 0.5 | 4.4 |
| Th | 3.6 ± 0.4 | 9.4 a | 14 ± 1.4 | 15 |
| Tl | 0.3 ± 0.1 | 0.4 | 0.7 ± 0.2 | 0.8 |
| U | 0.9 ± 0.3 | 1.5 | 4.1 ± 0.3 | 4.7 |
| V | 3.4 ± 0.9 | 84 b | 22 ± 6 | 27 |
| Zn | 30 ± 6 | 210 b | 66 ± 1 | 72 |

* Samples FS2224 and FS2233. Uncertainties are 1σ.

** Sample FS2228; a = beyond range of modern channel sands, but within range of medium to coarse sand separate of floodplain deposits; b = beyond range of medium to coarse sand separate of floodplain deposits; c = maximum value from this data set.

*** Samples FS2220, FS2223 (duplicate), FS2229, and FS2232 (duplicate). Uncertainties are 1σ.

**** Sample FS2227; a = beyond range of modern bulk floodplain deposits, but within range of fine sand to clay separates of floodplain deposits; b = beyond range of fine sand to clay separates of floodplain deposits; c = maximum value from this data set.

## Table 11
## Summary Statistics For Background Sediment Samples *

| Analyte | Number of Outliers | Minimum Value (ppm) | Median Value (ppm) | Mean Value (ppm) | Standard Deviation (ppm) | Maximum Value (ppm) | utl95** |
|---|---|---|---|---|---|---|---|
| Al | 0 | 740 | 5400 | 5020 | 2670 | 8400 | 11700 |
| As | 0 | <0.5 | 2 | 1.65 | 0.91 | 3.0 | 3.94 |
| Ba | 0 | 8 | 62.5 | 59.5 | 32.4 | 100 | 141 |
| Be | 0 | <0.08 | 0.68 | 0.59 | 0.32 | 1.1 | 1.40 |
| Ca | 0 | 180 | 1400 | 1450 | 747 | 2600 | 3340 |
| Co | 1 | 0.6 | 3 | 2.57 | 1.01 | 3.8 | 5.16 |
| Cr | 1 | 0.8 | 4.95 | 4.15 | 1.80 | 5.9 | 8.77 |
| Cu | 1 | 0.8 | 4.35 | 4.21 | 2.20 | 7.5 | 9.85 |
| Fe | 2 | 1400 | 8400 | 6970 | 2850 | 9600 | 14400 |
| K | 0 | 180 | 1250 | 1170 | 664 | 2200 | 2850 |
| K TOTAL | 1 | 22000 | 25500 | 25400 | 1800 | 29000 | 30000 |
| Mg | 0 | 170 | 1110 | 1030 | 509 | 1700 | 2310 |
| Mn | 1 | 46 | 240 | 241 | 97.2 | 380 | 490 |
| Na | 0 | 34 | 93 | 96.3 | 39.0 | 190 | 195 |
| Ni | 0 | <2 | 4.5 | 4.81 | 2.07 | 9 | 10.0 |
| Pb | 1 | <4 | 7.5 | 7.13 | 2.61 | 11 | 13.8 |
| Th | 1 | 0.9 | 5.9 | 5.24 | 2.28 | 8 | 11.1 |
| Th TOTAL | 1 | 3.3 | 15 | 12.7 | 4.68 | 18 | 24.7 |
| U | 1 | <0.3 | 0.6 | 0.58 | 0.27 | 1.0 | 1.29 |
| U TOTAL | 1 | 0.7 | 4.15 | 3.61 | 1.55 | 5.7 | 7.62 |
| V | 1 | 1.0 | 9.5 | 8.91 | 4.82 | 20 | 21.3 |
| Zn | 1 | 9 | 33.5 | 32.0 | 11.7 | 48 | 62.1 |

* Statistics presented for results of $HNO_3$ digestion procedures, except for K TOTAL, Th TOTAL, and U TOTAL, which were obtained from HF digestion procedures and are used for calculation of UTLs for specific radioactive isotopes (Table 12). Statistics were calculated after outliers presented in Table 13 were deleted, and analyses below the detection limit (DL) were considered as 1/2 DL. No values are presented for Cl, Sb, $SO_4$, Ta, and Tl because of the small number of analyses above DL (0-4).

** utl95 is a (.95,.95) UTL, computed using estimated mean and standard deviation and normal assumptions (i.e., selecting a "k-factor" appropriate for a sample of size 16 (0 outliers, k=2.523), 15 (1 outlier, k=2.566) or 14 (2 outliers, k=2.614). Then utl95 = mean + k*standard deviation).

**Table 12**
**Estimated Summary Statistics For Selected Radioactive Isotopes in Background Sediment Samples ***

| Isotope | Number of Outliers | Minimum Value (pCi/g) | Median Value (pCi/g) | Mean Value (pCi/g) | Standard Deviation (pCi/g) | Maximum Value (pCi/g) | utl95** |
|---|---|---|---|---|---|---|---|
| K-40 | 1 | 18.0 | 21.3 | 20.8 | 1.48 | 23.7 | 24.6 |
| Pa-231 | 1 | 0.01 | 0.06 | 0.06 | 0.02 | 0.09 | 0.12 |
| Ra-226 | 1 | 0.25 | 1.42 | 1.29 | 0.55 | 2.02 | 2.71 |
| Ra-228 | 1 | 0.36 | 1.64 | 1.39 | 0.51 | 1.97 | 2.70 |
| Th-228 | 1 | 0.36 | 1.64 | 1.39 | 0.51 | 1.97 | 2.70 |
| Th-230 | 1 | 0.25 | 1.42 | 1.29 | 0.55 | 2.02 | 2.71 |
| Th-232 | 1 | 0.36 | 1.64 | 1.39 | 0.51 | 1.97 | 2.70 |
| U-234 | 1 | 0.25 | 1.42 | 1.29 | 0.55 | 2.02 | 2.71 |
| U-235 | 1 | 0.01 | 0.06 | 0.06 | 0.02 | 0.09 | 0.12 |
| U-238 | 1 | 0.23 | 1.34 | 1.21 | 0.52 | 1.90 | 2.55 |

Notes:
* Statistics estimated using whole-sample values presented in Table 11 and correction factors presented in Table 14 (for K-40, Th-232, U-234, U-235, and U-238), or assumption of secular equilibrium with next higher parent isotope in decay chain (for Pa-231, Ra-226, Ra-228, Th-228, and Th-230). Statistics were calculated after outliers presented in Table 13 were deleted.
** utl95 is a (.95,.95) UTL. See footnote to Table 11.

**Table 13**
**Outliers in Background Sediment Data Set ***

| Sample Number | Sample Description | Analyte | Concentration (ppm) |
|---|---|---|---|
| FS2225 | black magnetite-rich sands | Co | 6 |
| | | Cr | 12 |
| | | Fe | 57000 |
| | | K TOTAL | 3600 |
| | | Mn | 1200 |
| | | Th | 14 |
| | | Th TOTAL | 130 |
| | | V | 66 |
| | | Zn | 300 |
| FS2226 | recent mud deposit | Cu | 12 |
| | | Pb | 16 |
| | | U | 1.6 |
| | | U TOTAL | 7.2 |
| FS2228 | prehistoric channel sands | Fe | 13000 |
| | | V | 20 |

Notes:
* Outliers only calculated for $HNO_3$ digestion, except for values labeled "TOTAL", which were obtained using HF digestion. Outliers identified as values that would inflate the estimate of the mean by more than 10%, except for the K TOTAL value for sample FS2225, which was anomalously low in comparison to the other samples.

**Table 14**
**Correction Factors Used to Estimate Concentrations of Selected Radioactive Isotopes ***

| Isotope | Specific Activity (pCi/g) | Natural Abundance (%) | Correction Factor (pCi/g per ppm) |
|---|---|---|---|
| K-40 | $6.99 \times 10^{6}$ | 0.0117 | $8.1736 \times 10^{-4}$ |
| Th-232 | $1.09 \times 10^{5}$ | 100 | $1.092 \times 10^{-1}$ |
| U-234 | $6.23 \times 10^{9}$ | 0.0057 | $3.55 \times 10^{-1}$ |
| U-235 | $2.16 \times 10^{6}$ | 0.710 | $1.53 \times 10^{-2}$ |
| U-238 | $3.36 \times 10^{5}$ | 99.28 | $3.34 \times 10^{-1}$ |

Notes:
* Whole-sample values of K, Th, and U presented in Table 11 were multiplied by these correction factors to provide estimates of activity in background sediment samples. Values from Installation Work Plan for Los Alamos National Laboratory Environmental Restoration Project.